A close-up photograph of a metallic fuel assembly component, likely a fuel rod or spacer grid, showing a circular opening. The metal has a textured, slightly grainy appearance with some darker spots, possibly from oxidation or manufacturing. The lighting is dramatic, highlighting the edges and the interior of the opening.

ZIRAT17 SPECIAL TOPIC REPORT

High Strength Nickel Alloys
for Fuel Assemblies

High Strength Nickel Alloys for Fuel Assemblies

Authors

Alfred Strasser

Aquarius Service Corp., Sleepy Hollow, NY, USA

Peter Ford

Rexford, NY, USA



A.N.T. INTERNATIONAL®

© October 2012

Advanced Nuclear Technology International

Analysvägen 5, SE-435 33 Mölnlycke

Sweden

info@antinternational.com

www.antinternational.com



Ecolabelled printed matter, 441 799

Disclaimer

The information presented in this report has been compiled and analysed by Advanced Nuclear Technology International Europe AB (ANT International®) and its subcontractors. ANT International has exercised due diligence in this work, but does not warrant the accuracy or completeness of the information.

ANT International does not assume any responsibility for any consequences as a result of the use of the information for any party, except a warranty for reasonable technical skill, which is limited to the amount paid for this assignment by each ZIRAT/IZNA programme member.

Contents

1	Application of alloys in reactor internals (Alfred Strasser)	1-1
1.1	Introduction	1-1
1.2	Development of nickel alloy applications for fuel assemblies	1-2
1.3	PWRs	1-3
1.3.1	Westinghouse	1-3
1.3.2	AREVA	1-6
1.3.3	Mitsubishi (MHI) reloads	1-9
1.4	BWRs	1-10
1.4.1	Global Nuclear Fuel (GNF)	1-10
1.4.2	AREVA	1-12
1.4.3	Westinghouse	1-15
2	Unirradiated alloy physical and mechanical properties (Alfred Strasser)	2-1
2.1	Introduction	2-1
2.2	Physical properties	2-1
2.2.1	Composition	2-1
2.2.2	Alloy 625	2-2
2.2.3	Alloy 718	2-2
2.2.4	Alloy X-750	2-3
2.2.5	Alloy A286	2-4
2.3	Mechanical properties	2-4
2.3.1	Alloy 625	2-4
2.3.2	Alloy 718	2-7
2.3.3	Alloy X-750	2-9
2.3.4	Alloy A286	2-12
3	Physical metallurgy of non-irradiated high-strength, high-nickel alloys (Peter Ford)	3-1
3.1	Introduction	3-1
3.2	Phases present in high-strength, high-nickel alloys	3-4
3.3	Strengthening mechanisms and heat treatments for specific alloys	3-11
3.3.1	Alloy 286	3-13
3.3.2	Alloy 718	3-16
3.3.3	Alloy 625	3-20
3.3.4	Alloy X-750	3-21
3.4	Grain boundary effects	3-26
3.4.1	Grain boundary sensitization	3-26
3.4.2	Grain boundary plasticity	3-28
4	Fabrication of alloys (Alfred Strasser)	4-1
4.1	Introduction	4-1
4.2	Ingot melting	4-2
4.3	Hot forming	4-9
4.4	Cold forming	4-9
4.5	Heat treatment	4-15
4.6	Joining	4-15
4.7	Surface treatment	4-15

5	Corrosion of high-strength, high-nickel alloys in LWR reactor internals (Peter Ford)	5-1
5.1	Introduction	5-1
5.2	Parametric dependencies of EAC in high-strength, high-nickel alloys	5-6
5.2.1	Alloy 286 (UNS designation S66286)	5-6
5.2.2	Alloy X-750 (UNS designation NO7750)	5-7
5.2.3	Alloy 718 (UNS designation N07718)	5-16
5.2.4	Alloy 625 (UNS designation N06625)	5-18
5.3	Summary	5-19
6	Effects of composition on microstructure and properties (Alfred Strasser)	6-1
6.1	Effect of alloying elements	6-1
6.1.1	Nickel and niobium	6-1
6.1.2	Carbon and chromium	6-2
6.1.3	Molybdenum	6-4
6.2	Effect of impurities	6-4
6.2.1	Boron and zirconium	6-4
6.2.2	Phosphorus and boron	6-5
6.2.3	Calcium	6-6
6.2.4	Lead, bismuth, silver, selenium	6-6
7	Effects of irradiation on microstructure and properties (Alfred Strasser)	7-1
7.1	Introduction	7-1
7.2	Crystal structure	7-1
7.3	Microstructure and mechanical properties	7-2
7.3.1	Introduction	7-2
7.3.2	Alloy 718	7-3
7.3.3	Alloy X-750	7-8
7.3.4	Alloy 625	7-11
7.4	Transmutations	7-12
7.4.1	Boron	7-12
7.4.2	Nickel	7-14
8	In-reactor performance of high nickel alloy fuel assembly components (Alfred Strasser)	8-1
8.1	Introduction	8-1
8.2	Spacer grids	8-3
8.2.1	PWRs	8-3
8.2.2	BWRs	8-4
8.3	Upper nozzle – PWRs	8-6
8.3.1	Hold-down springs	8-6
8.3.2	Hold-down screws	8-9
8.4	BWR channel fastener screw	8-13
9	Conclusions relevant to LWRs	9-1
9.1	Applications (Alfred Strasser)	9-1
9.2	Unirradiated physical and mechanical properties (Alfred Strasser)	9-1
9.3	Physical metallurgy of unirradiated alloys (Peter Ford)	9-1
9.4	Fabrication of alloys (Alfred Strasser)	9-2
9.5	Corrosion of alloys (Peter Ford)	9-3
9.6	Effects of composition on microstructure and properties (Alfred Strasser)	9-6
9.7	Effects of irradiation on microstructure and properties (Alfred Strasser)	9-6
9.8	Performance of high nickel alloy components in fuel assemblies (Alfred Strasser)	9-7
10	References	10-1

Appendix A – History of nickel alloy development and the rationale for their choice in LWR applications (Peter Ford)	A-1
Appendix B – Effect of environment on unstable crack propagation and fracture resistance (Peter Ford)	B-1
B.1 Introduction	B-1
B.2 High temperature water	B-3
B.3 Low temperature, hydrogenated water	B-4
B.3.1 Material	B-5
B.3.2 Environment	B-5
B.3.3 Stress/strain rate	B-6
Appendix C – Corrosion of <i>ductile</i> austenitic alloys in LWR reactor internals (Peter Ford)	C-1
C.1 Introduction	C-1
C.2 General corrosion of austenitic stainless steels and high-nickel alloys	C-2
C.2.1 Thermodynamic considerations	C-2
C.2.2 Oxidation rates for austenitic stainless steels and nickel-base alloys	C-9
C.3 Environmentally-assisted cracking of ductile austenitic alloys in LWRs	C-10
C.3.1 Background	C-10
C.3.2 Chronology of events	C-12
C.3.3 Mechanistic understanding of EAC in ductile austenitic alloys in LWRs	C-16
C.3.4 Parametric dependencies and life prediction of EAC in ductile austenitic alloys in LWR primary systems.	C-26
Appendix D – References	D-1
Nomenclature	
Unit conversion	

1 Application of alloys in reactor internals (Alfred Strasser)

1.1 Introduction

The selection of materials for the reactor internals depend on their adequate and hopefully superior performance in the service that they will be exposed to. At least three physical and metallurgical issues need to be considered when choosing alloys for specific applications in reactors:

- *Mechanical and physical properties* (e.g. yield and tensile strengths, ductility, fracture resistance, coefficient of thermal expansion) which ensure that structural integrity and functionality are maintained under the specific reactor operating conditions over the licensed life of the component. Fracture resistance (or toughness) which may be impaired by radiation hardening, or thermal aging, is of particular regulatory concern since these embrittlement modes may lead to unstable crack propagation under specific conditions of crack depth and tensile stress.
- *Resistance to environmentally-assisted degradation* that may occur relatively slowly over time. This may be associated with corrosion, both uniform and localized, assisted by stress, galvanic action, or changes in the surface structure of the alloys. Radiation has significant effects on the metallurgical structure of materials, their properties, their dimensions and can influence corrosion processes, particularly stress corrosion. The environments may be severe involving, in some cases, high radiation fluxes, stresses or chemical concentrations that can occur in occluded areas associated with crevices or on heat transfer surfaces.
- *Ability to fabricate* homogeneous, reproducible high quality materials.

These factors have been extensively discussed in other ANT International reports on zirconium alloys and their application to fuel assemblies in the ZIRAT program and the main structural components in water cooled reactors in the LCC program and their reports are referenced wherever additional detailed information could be of value.

The intent of this report is to provide information on the high strength nickel (Ni) alloys used primarily in the structural components of the fuel assembly and the information is applicable to some of the core internals. The report includes their physical metallurgy, development, fabrication, application and performance. These alloys contain significant amounts of Ni and chromium (Cr), and the most frequently used alloys contain >50% Ni. They meet the criteria listed above to a very high degree, particularly with their high strength and oxidation resistance; however, every material has its limitations and this report intends to discuss both the advantages and disadvantages of these alloys.

The report is structured to lead the reader logically from the applications of the alloys in Chapter 1 to their performance in Chapter 8. Chapter 2 provides the basic alloy properties and then leads to a detailed discussion of their complex metallurgical structure in Chapter 3 that describes the variety of phases that they may contain and the relationship of heat treatments to their presence. Having established the vocabulary for their metallurgical structure, Chapter 4 describes the various fabrication methods and their effect on the properties of the alloys starting with ingot melting. Having described the variety of characteristics that the alloys may have, Chapter 5 discusses how these characteristics, primarily their microstructure, can react to their environment, specifically to stress corrosion cracking (SCC) one of the most significant performance adversaries to these alloys. Chapter 6 discusses the effect of variances in the alloying content and impurity levels on properties. Chapter 7 describes the effect that irradiation has on the structure and the properties of the alloys including the effects that transmutation of some of the elements may have. Chapter 8 summarizes all the reported failures of the fuel assembly components, made of these alloys, which have occurred, their causes and remedies. Chapter 9 provides conclusions for the various topics covered and Chapter 10 is an extensive list of references that can provide more details. Three Appendices provide some additional details: Appendix A describes the history of the nickel alloy development, Appendix B provides a tutorial for fracture propagation, an important topic for the failure mechanisms of these components, and Appendix C discusses the basic of environmental assisted cracking, including stress corrosion cracking, in LWRs.

1.2 Development of nickel alloy applications for fuel assemblies

Nickel alloys were developed for high temperature applications long before nuclear applications, in order to take advantage of their excellent strength at high temperatures. One obvious disadvantage for nuclear core applications is that the high Ni alloys do not meet the low neutron cross section criterion for the core and as a result, essentially all of their applications are on the edge of, or on the outside of the core. The two exceptions are the spacer grids used in some of the fuel elements and the cladding used for some of the PWR absorber rods. The Ni alloy spacer grids replace low absorption cross section, weaker, zirconium (Zr) alloy grids where the service requirements exceed the margin to the Zr alloy mechanical property limits. The high Ni absorber rod cladding is used in some designs instead of stainless steels, presumably as a higher strength material to resist absorber swelling, but since the absorber rod is designed to have a high absorption cross section, the high Ni content can actually add a slight advantage to its nuclear performance.

Most of the high Ni alloys in use today were developed over 50 years ago for high temperature applications, primarily for aircraft gas turbines and subsequently power plant steam turbines, and the oil and gas exploration industry, applications that are still very active. The Alloys 718, X-750 and 625, all >50% Ni, are the most frequently used by the nuclear industry today and they were developed by the Huntington Alloy Co. funded by the International Nickel Company. The family of alloys has been marketed under the trade name of INCONEL and in this report they will be noted as Alloy 718, Alloy X-750 and Alloy 625.

The A286 alloy was also developed commercially for similar high temperature applications, but has a lower Ni content of 24-27%. While it has some good high temperature properties, its initial use by the nuclear industry has declined as discussed later.

The high strength development of the above alloys falls into two categories: precipitation hardening and solution hardening. The Alloys 718, X-750 and A286 are precipitation hardened by heat treatments that dissolve and then precipitate intermetallic compounds that increase the strength of the multiphase material.

The Alloy 625 is hardened by alloying elements that are dissolved in its matrix and thereby provide the higher strength of the material. Details of these heat treatments and their effects on the metallurgical structure are discussed in Chapter 3.

The austenitic Type 300 series stainless steels (18% Cr, 8% Ni) are used extensively in reactor internals, but have lower strengths and may not qualify for the high strength applications considered in this report. Exceptions are very limited applications of Type 316 stainless steels that have been cold worked to increase their mechanical properties.

The applications of the high strength alloys in PWR and BWR fuel assemblies in the current designs of each fuel vendor are summarized in the sections that follow, including comments on the design modifications and the reasons for their changes. Detailed discussions of the failures of these components in the fuel assembly are given in Chapter 8.

1.3 PWRs

1.3.1 Westinghouse

1.3.1.1 Westinghouse reloads for Westinghouse NSSS

Grids

The material applications in the various Westinghouse fuel assembly designs are similar from one design to the other, including the 15x15, 17x17, OFA and Robust Fuel designs. The high nickel alloy applications in these designs are shown on Figure 1-1.

Originally all of the grids were made of high Ni alloys until sufficient confidence was developed to change to the lower neutron capture cross section Zircaloy-4 grids with Alloy 718 springs. The performance of the original grids as well as the modified bimetallic grids was excellent. The major advantage of the change was increased reactivity leading to lower enrichment requirements and the attendant decrease in coolant activation due to cobalt transport from the Ni alloys. The improved performance ZIRLO alloy replaced Zircaloy-4 for the current designs, but maintained the bimetallic grid design.

2 Unirradiated alloy physical and mechanical properties (Alfred Strasser)

2.1 Introduction

The as fabricated, unirradiated properties of the alloys are summarized in this Chapter. The data are nominal values provided by standards, handbooks and the material suppliers to provide an overview of the alloy characteristics. The majority of the property data are from the major Ni alloy producer, [Special Metals, 2004a, b, 2006 and 2007]. The properties directly applicable to components used in reactors are given in subsequent sections. Specifically, the effects of heat treatment methods on properties is discussed in Chapter 3, the effects of fabrication methods in Chapter 4, the effects of the service environment (stress, coolant, radiation) in Chapter 5, the effects of composition in Chapter 6 and the effects of irradiation in Chapter 7. These must be taken into account in the design of the components.

Ultimately, it is the materials specification of the fuel vendor that determines the alloy properties and their subsequent effect on the performance of the components. These specifications are generally proprietary hence are not included in this report; however, they are an important area to audit by the users of the components, in order to assure that they have been adequately qualified.

2.2 Physical properties

2.2.1 Composition

The composition of the alloys that have been and are being used in fuel assemblies are given in Table 2-1. Alloys 600, and 690 are not used in fuel assemblies any more, but their composition is given here as a reference.

Table 2-1: Composition of high Ni alloys (weight %).

Alloy	Ni	Cr	Fe	C max	Mo	Nb	Ti	Al	V	Si max	Cu max	Mn max	P max	S max	B max	Co* max
A286	24.0-27.0	13.5-16.0	Bal.	0.08	1.0-1.75	-	1.90-2.30	.035 max	0.10-0.50	1.00	-	2.0	0.025	0.025	0.003-0.010	
600	72.0 min	14.0-17.0	6.0-10.0	0.05	-	-	-	-	-	0.50	0.50	1.0	0.1	0.015	-	0.5
625	58.0 min	20.0-23.0	<5.0	0.10	8.0-10.0	3.15-4.15 (+ Ta)	0.4 max	0.4 max	-	0.50	0.30	0.5	0.015	0.015	0.020	
690	58.0 min	27.0-31.0	7.0-11.0	0.05	-	-	0.5	0.5	-	0.50	0.50	0.5	0.025	0.015	-	0.1
718	50.0-55.0	17.0-21.0	Bal.	0.08	2.80-3.30	4.75-5.50 (+ Ta)	0.65-1.15	0.20-0.80	-	0.35	0.30	0.35	0.015	0.015	0.006 max.	
X-750	70.0 min	14.0-17.0	5.0-9.0	0.08	-	0.70-1.20 (Ta)	2.25-2.75	0.40-1.00	-	0.50	0.50	1.0	0.008	0.010	-	
800	30-35	19-23	>39.5	0.10			0.15-0.60	0.15-0.60		0.10	0.75	1.5	0.03	0.03		

* Co is generally specified as 0.05% max. for high Ni alloys.

ANT International, 2012

The cobalt (Co) content of standard commercial Ni alloys is rarely analyzed and reported and varies widely depending on the amount of and Co content of the scrap recycle used and when specified can be as high as 1.0% maximum. Since the content of components with this level of Co in contact with the coolant is undesirable, a lower level of 0.05% maximum is generally specified.

The boron (B) content is often unspecified or analyzed and this is another element that can have a negative effect on mechanical properties due to its transformation to helium (He) and lithium (Li) in an irradiation field as discussed in Chapter 7. Additional discussion of the effect of impurities on the material properties is given in Chapter 6.

The unirradiated properties of the alloys currently used in fuel assemblies, Alloys 625, 718 and X-750, are summarized in the following sections. However, an extensive review of the properties of the other alloys can be found in ANT International's report by P. Scott, P. Combrade and P. Ford, "Environmentally-Assisted Degradation of Nickel-Base Alloys in LWRs", September, 2011 [Scott et al, 2011] on the ex-core application of these alloys.

2.2.2 Alloy 625

Melting Range 1290-1350°C

Density 8.44 g/cc

Thermal Properties Expansion coefficient, thermal conductivity, specific heat is in Table 2-2.

Electrical Properties Electrical resistivity is in Table 2-2.

Magnetic Properties Magnetic permeability: 1.0006 at 200 oersteds (15.9 kA/m)

Table 2-2: Alloy 625 thermal and electrical properties.

Temperature		Mean linear ^{a)} expansion μm/μm • °C	Thermal conductivity W/m • °C	Specific heat J/Kg °C	Electrical resistivity μΩ - cm
°F	°C				
70	21	-	9.8	402	129
100	38	-	10.1	410	130
200	93	12.8	10.8	427	132
400	204	13.1	12.5	456	134
600	316	13.3	14.1	481	135
800	427	13.7	15.7	511	136
1000	538	14.0	17.5	536	138

^{a)} Mean coefficient of linear expansion from 70°F to temperature shown.

ANT International, 2012

2.2.3 Alloy 718

Melting Range 1280-1336°C

Density 8.22 g/cc

Thermal Properties Expansion coefficient, thermal conductivity, specific heat is in Table 2-3.

Electrical Properties Electrical resistivity is in Table 2-2.

Magnetic Properties Magnetic permeability: 1.0011 (aged) at 200 oersteds (15.9 kA/m)

Table 2-3: Alloy 718 thermal and electrical properties (Annealed and aged^{a)})

Temperature		Mean linear expansion ^{b)} μm/μm • °C	Thermal conductivity ^{a)} w/m • °C	Specific heat J/Kg °C	Electrical resistivity μΩ - cm
°F	°C				
70	21	-	11.4	435	121
200	93	13.2	12.6		122
400	204	13.6	14.4		125
600	316	14.0	16.2		128
800	427	14.4	17.9		129
1000	538	14.6	19.6		131

^{a)} Annealing was 1800°F/1 hr, aging was 1325°F/8 hr, F.C. 20°/hr to 1150°F, held at 1150°F for total aging time of 18 hr. Conductivity calculated from resistivity values.
^{b)} Mean coefficient of linear expansion from 70°F to temperature shown.

ANT International, 2012

2.2.4 Alloy X-750

Melting Range 1393-1427°C

Density 8.28 g/cc

Thermal Properties Expansion coefficient, thermal conductivity, specific heat is in Table 2-4.

Electrical Properties Electrical resistivity is in Table 2-4.

Magnetic Properties Magnetic permeability: 1.0035 (aged) at 200 oersteds (15.9 kA/m)

Table 2-4: Alloy X-750 thermal and electrical properties^{a)}.

Temperature		Mean linear expansion ^{a)} μm/μm • °C	Thermal conductivity W/m • °C	Specific heat J/Kg °C	Electrical resistivity μΩ - cm
°F	°F				
70	21	-	11.8	431	122
200	93	12.6	12.8	457	123
400	204	13.0	14.1	486	124
600	316	13.5	15.7	503	127
800	427	14.0	17.3	524	128
1000	538	14.6	18.9	545	130

^{a)} Mean coefficient of linear expansion from 70°F to temperature shown.

ANT International, 2012

3 Physical metallurgy of non-irradiated high-strength, high-nickel alloys (Peter Ford)

3.1 Introduction

A short historical perspective of the development of nickel-base alloys and the rationale for their use in Light Water Reactors (LWR) is given in Appendix A. This acts as a background to the focus in this Chapter on the physical metallurgy of the non-irradiated high-strength Alloys X-750, 718, 625 and A286, with specific attention to; (a) the metallurgical structure of the alloys; (b) the second phase particles present as a function of the various heat treatments, and; (c) their effect on the mechanical properties. These interactions are of importance since they impact on the failure of the high-strength, high-nickel alloys by environmentally assisted cracking (EAC) in reactor fuel assemblies and related internals in LWRs.

The topic of EAC is discussed in Chapter 5 while the effect of irradiation on the structure of these alloys is covered in Chapter 7.

The compositions of the alloys of interest are compared with those of Type 304 stainless steel and Alloy 600 in

Table 3-1 where it is seen that all the alloys have a significant chromium content (13.5-23%), which confers good general corrosion resistance in LWR coolant, and nickel contents varying from 8-10.5% in Type 304 stainless steel to a 72% minimum in Alloy 600.

Table 3-1: Compositions (weight %) of Type 304 stainless steel and Alloys 600, 286, 718, 625, and X-750.

Alloy	Type 304 SS	Alloy 286	Alloy 718	Alloy 625	Alloy X-750	Alloy 600
UNS/W.Nr	S30400	S66286/ 1.4980	N07718/ 2.4668	N06625/2.4856	N07750/2.4669	N06600/2.4816
Wt %						
Ni	8-10.5	24-27	50-55	58 min	70 min	72 min
Cr	18-20	13.5-16	17-21	20-23	14-17	14-17
Fe	66-74	Bal (approx 57)	Bal (approx 19)	5.0 max	5-9	6-10
Nb +Ta			4.75-5.5	3.15-4.15	0.7-1.2	
Mo		1-1.75	2.8-3.3	8-10		
Ti		1.9-2.35	0.65-1.15	0.4 max	2.25-2.75	
Al		0.35 max	0.2-0.8	0.4 max	0.4-1.0	
Co			1.0 max	1.0	1.0 max	0.1 max
C max	0.08	0.08	0.08	0.1	0.08	0.05
Mn max	2.0	2.0	0.35	0.5	1.0	1.0
Si max	1.0	1.0	0.35	0.5	0.5	0.5
P max	0.045	0.025	0.015	0.015		0.1
S max	0.03	0.025	0.015	0.015	0.01	0.015
B		0.003-0.01	0.006 max	0.02		
Cu max			0.3	0.3	0.5	0.5
V		0.1-0.5				

ANT International, 2012

All of the targeted high-strength alloys have a matrix comprising a Face Centred Cubic (FCC) austenite phase (γ) (denoted by the blue shading in Figure 3-1); this dominant phase is to be expected given the high nickel content that stabilizes the austenite. The austenite phase becomes metastable at nickel contents lower than approximately 15-25% (depending on the chromium content); under these conditions increasing amounts of body centred cubic (bcc) ferrite are in equilibrium with the austenite, (as illustrated by the yellow shaded region in Figure 3-1). This is especially the case if the chromium content is maintained $> 10\%$ since this alloying addition stabilizes the ferrite structure.

This balance of the counteracting effects of chromium and nickel to control the austenitic and ferritic phase stabilities is the basis of not only the classical austenitic stainless steels (Type 304, 316, etc.), but also the duplex (Type 308, 309, etc) and cast stainless steels (CF8, CF8M, etc.), the high strength martensitic (A-410) and precipitation hardened stainless steels. Examples of the last category include Alloy 286, one of the targeted alloys in this report. Decreasing the nickel content to 3-5% Ni, while maintaining the chromium content in the range of 13-25% ensures the fully ferritic structure (as depicted by the green shaded region in Figure 3-1) found in the ferritic stainless steels (A-430, A-405). Ultimately, as both the chromium and nickel contents are lowered to values less than 1-2%, the microstructures are controlled by the thermal and athermal transformations from austenite (that is stable at higher temperatures) to ferrite and various intermetallics and compounds such as cementite, martensite and bainite found in carbon and low alloy steels (LAS). As might be expected the management of this diversity of phase stabilities and formation of second phase particles, etc. leads to the possibility of a wide range of mechanical (and physical) properties.

These microstructural and mechanical strength developments have been extensively discussed [Ford, 2006] in other ANT International reports addressing carbon and low alloy steels [Ford & Scott, 2008], stainless steels, [Ford et al, 2010] and the ductile nickel-base alloys [Scott et al, 2011].

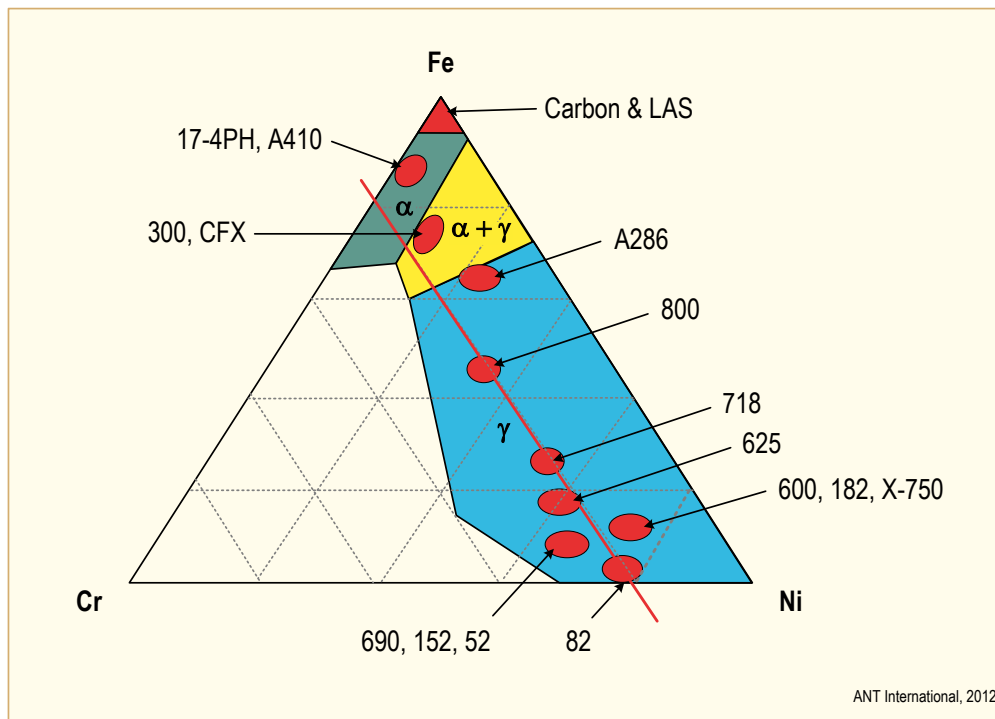


Figure 3-1: Ternary diagram for the Fe-Cr-Ni system at 400°C illustrating the compositions of the main structural alloys in water cooled reactors and the thermodynamically stable austenitic (γ) and ferritic (α) crystal structures denoted by the blue and green areas respectively. The austenite phase in the yellow region is metastable leading to a wide range of austenitic, ferritic, martensitic and duplex stainless steels. Note that the austenite phase is stable for the alloys of current interest (X-750, 718, 625 and A-286), with chromium contents around 20% (denoted by the red line).

The strengthening mechanisms relevant to the high-strength, high-nickel alloys of interest depend on the hindering of dislocation movement by a combination¹ of the following processes;

- 1) Solid solution strengthening associated with alloying elements that are larger or smaller than the primary matrix atoms. This strengthening is caused by lattice distortion that increases with atomic size mismatch between the matrix atoms and the alloying additions. There is a limit to this effect since larger degrees of atomic size mismatch (approximately 10%) are accompanied by a decrease in alloying element solubility. This hardening mechanism dominates in the ductile Type 304 stainless steel and Alloy 600.

Examples of the solute atoms that confer solid solution strengthening in high-nickel alloys are chromium and iron. Alloying additions such as aluminium may also decrease the stacking fault energy resulting in the formation of extended partial dislocations that inhibit dislocation cross slip and, thereby, the ability of the dislocation to bypass obstacles by moving onto a new slip plane. Short range ordering, or clustering of the solute atoms, is a related strengthening mechanism and is observed with additions of chromium, aluminium, molybdenum and tungsten.

- 2) Work hardening by cold or warm deformation at a temperature below that at which recovery can occur. Dislocation movement in this case is hindered by the increasing amount of dislocation tangles, the details of which depend on the number of slip systems, the temperature, (which encourages dislocation climb around obstacles), stacking fault energies, etc.. Plastic deformation is also used in the high-nickel alloys in conjunction with various high temperature heat treatments in order to refine the microstructure, or to homogenize the cast structure at temperatures circa. 1232°C (2250°F).
- 3) High angle grain boundaries that can hinder the transference of dislocation movement between adjacent grains. For many alloys the yield stress increases with decreasing grain size, which, as discussed later, can be controlled in nickel-base alloys by attention to the melting practice and the extent of plastic deformation before high-temperature heat treatment.
- 4) Hardening due to the presence of second phase precipitates in the metal. Such a precipitation hardening mechanism dominates in Alloys 718 and X-750, and is a significant factor in Alloys 286 and 625 that were originally designed as solid solution hardened materials. This is a particularly complex strengthening mechanism that depends on the size, spacing and mechanical properties of the precipitate, the state of coherency between the precipitate and matrix, the extent of short range order, etc.. The physical metallurgy of precipitation hardened nickel-base alloys has been addressed in a number of books [Durand-Charre, 1997], [Sims et al, 1987], [Geddes et al, 2010], [Davis, 2007] as well as papers in technical journals, and bulletins from the alloy suppliers (e.g. www.specialmetals.com). The alloying elements that can give rise to precipitation hardening in high-nickel alloys are, primarily, Al, Ti and Nb (+Ta), which form precipitates such as Ni₃Al, (γ'), and Ni₃Nb, (γ''). (Note that these are simplified compositions since, as discussed momentarily, other elements are soluble in these structures)

¹ Note that although one of these strengthening mechanisms may be dominant in a particular alloy, there can be significant contributions from the other mechanisms.

4 Fabrication of alloys (Alfred Strasser)

4.1 Introduction

The primary producers of Ni alloys from the ingot to the semi-finished product stage in the USA are Allvac, Carpenter Technology and Special Metals Co., and Aubert & Duval in France. These companies produce the alloys to the proprietary process and materials specifications of the fuel vendors. Strips for applications such as spacers are rolled to an intermediate size and are rolled to final thickness by a fuel vendor subcontractor. Wire for helical springs is provided to another fuel vendor subcontractor, a spring manufacturer, for producing the final product. The same sequence is followed for bar stock that is provided to a contractor for final machining or sizing. The fuel vendors should audit the alloy producers to assure that their procedures are followed.

The fabrication processes and conditions used to make the high strength Ni alloys have a significant effect on the properties and the performance of the components made from these materials, an effect that is applicable from the initial ingot melting to the finished product. The relationship between the fabrication processes and the ultimate material properties is reasonably flexible, so that the fabrication processes can be optimized for the intended service. Most of these alloys were developed for high temperature use in aircraft gas turbines operating at about 650°C (1200°F) and above, where maximum strength, creep and oxidation resistance are of prime importance. They are also used in the oil, gas and chemicals industry where corrosion resistance as well as high strength are most important. The reactor applications are for service up to about 400°C (750°F) at high strength and resistance to fatigue and stress corrosion cracking (SCC). The optimum fabrication conditions are somewhat different for each of these applications. There are an extensive number of specifications that have been developed for these alloys including their fabrication methods, primarily for the aircraft industry by the Aerospace Materials Standards (AMS) and by the American Society for Testing and Materials (ASTM). Specifications have been issued in Europe by the International Organization for Standardization (ISO), and in Germany by the Deutsches Institut für Normung (DIN) and TÜV. However, the only specification that applies to any of the high strength alloy nuclear components is the one that the fuel vendor is using, which may be one of the existing specifications, a modified one or one written by the vendor.

According to both the US metal suppliers and users there are no specifications or QA requirements for these alloys that are specific to nuclear applications. The only fabrication processes that have been qualified are those for the aerospace industry and the US Navy. The low level of process control has prompted one knowledgeable person in this industry to say that he would expect that material bought to ASME specifications would have a 75 to 80% probability of having some form of a gross defect.

This pessimistic view of the current state of the industry is further influenced by the current supply and demand situation. Large lots of Alloy 718 are provided primarily for the turbine industry, but the demand, and therefore the production, for Alloy X-750 is limited. As a result the timely supply to the fuel vendors is unlikely to be qualified for their specification, nor necessarily processed to their specification, if there is one. The fabrication processes may vary from heat to heat, and this is reflected in the variability of results in the performance of samples tested in ex-reactor research programs as well as in-reactor performance of components. This applies to both alloys, but particularly to the smaller lots of Alloy X-750 [Morra, 2012]. The pessimistic view reported here may not apply to every alloy vendor, user or every lot of material; however, it calls for a meticulous and significantly improved review and upgrading of the applicable specifications, process qualification, process control, quality control and quality assurance of the fabrication and the final product of the high strength Ni alloys for nuclear applications.

Comments to follow on the fabrication process are applicable to all of the high strength nickel alloys. The high strength that resists deformation in the performance of these materials also resists deformation during fabrication. In the cold reduction processes the materials strain harden readily, as shown on Figure 4-1, and require frequent annealing between reduction steps. Powerful equipment is needed for hot working processes in order to achieve the desired reductions. Uniformly high temperatures and deformation processes need to be maintained in order to achieve a uniform structure and properties.

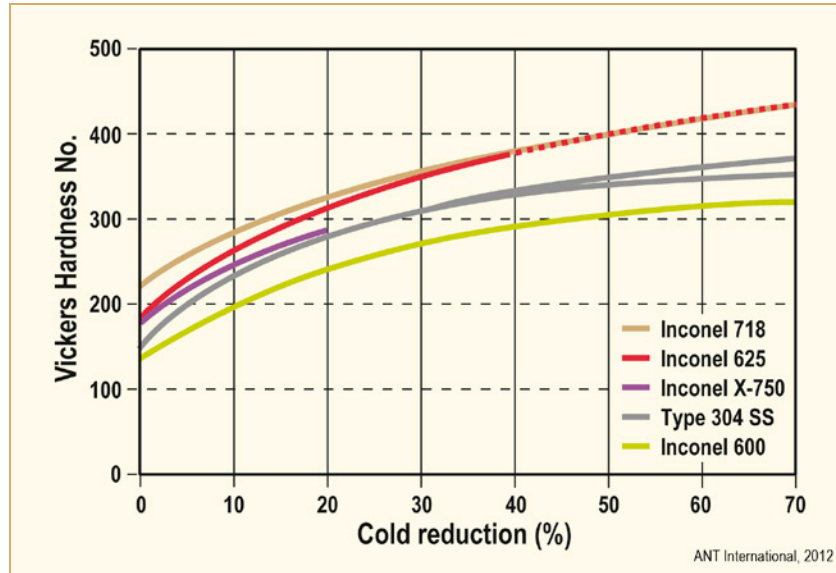


Figure 4-1: The effect of cold work on hardness.

Significant fabrication process parameters that could affect the performance of the alloys are discussed in the following subsections with the exception of the effects of various heat treatment processes on properties that are described in Chapter 3 and 5. Some of the fabrication data are from the brochures of the major fabricator of nickel alloys, such as references [Special Metals, 2006, 2007, 2004a and b], and are not to be interpreted as specifications.

4.2 Ingot melting

Vacuum melting was applied to the high strength Ni alloys in the early 1950's in order to improve the performance of gas turbines in the aircraft industry, previously made from air melted material. Vacuum induction melting (VIM) followed by vacuum arc melting (VAR) of a consumable electrode produce a more homogeneous material, free of unwanted impurities. This process sequence is recommended for nuclear components [Morra, 2012]. The improved compositional and microstructural control provides significantly improved, reproducible mechanical strength, ductility and oxidation resistance.

The means by which vacuum melting achieves improved properties can be summarized as follows:

- Removal of oxygen, nitrogen and hydrogen from the melts, which would form non-metallic inclusions if present,
- Evaporation of undesirable trace elements,
- De-carburization by oxygen without formation of other undesirable reaction products,
- Produce low carbon products,
- Control the homogeneity of the metallurgical structure.

Several of the alloying elements have a great affinity for oxygen and nitrogen and would form oxides and nitrides that would not be removed by air melting. This is particularly true of titanium (Ti) and aluminium (Al), two key alloying elements in the age hardening alloys that are instrumental in forming the hardening phase, γ' .

Two impurities that need to be controlled are cobalt (Co) and boron (B). Control of Co, preferably below 0.1%, will reduce coolant activity transfer particularly from such high surface area components as spacer grids. The Co content is introduced originally in combination with the Ni ore and is claimed to be difficult to separate. A secondary source comes from recycled material which may or may not be carefully controlled. Alloy 718 appears to be particularly high in Co, ranging from about 0.5% to 1.0% and if not lowered, would be one of its disadvantages.

Additions of B are made for aerospace applications for improved high temperature mechanical properties and as a deoxidant in ingot melting. In nuclear applications, however, it transforms to helium and lithium and has detrimental effects on properties. Evaluation of irradiated Alloys 625 and X-750 with various B contents suggest that it should be <10 ppm. Detailed discussion is provided in Section 7.4.1.

Maximum levels for Co and B do not exist in current specifications, unless they are included in the fuel vendors' specifications to the alloy supplier.

Of the undesirable trace elements, bismuth (Bi) has been identified as the most damaging, followed by tellurium (Te), selenium (Se) and lead (Pb). At the level of 0.2% Bi, the creep ductility of cast alloys can be reduced by 20% or more. Bi, as well as Pb has an adverse effect on the hot working capability of the alloys by forming low melting compounds at the grain boundaries. Silver (Ag) and tin (Sn) impurities appear to have little effect. The effects of various elements are discussed in Chapter 6.

The effect of sulphur (S) is particularly deleterious to nickel alloy properties and hot workability. Sulphur must be controlled in the raw materials used to make-up the ingot and has also been controlled through the careful, minor additions of magnesium (Mg), calcium (Ca), zirconium (Zr), cerium (Ce) and yttrium (Y) that combine with and immobilize sulphur [Sinha et al, 2005].

The reaction of carbon with oxygen to form CO to reduce carbide formation is feasible only under the reduced partial pressure of CO in the vacuum melting process [Franz, 2006].

The magnetic stirring capability and longer holding times during vacuum melting promote the good homogeneity and reproducibility of the product.

The VIM furnaces operate at pressures in the range of 10^{-3} to 10^{-2} mbar with leakage rates down to 5×10^{-3} mbar/sec. The larger capacity VIM degassing and pouring furnace is shown in Figure 4-2.

5 Corrosion of high-strength, high-nickel alloys in LWR reactor internals (Peter Ford)

5.1 Introduction

This chapter addresses environmentally-assisted degradation of the high-strength, high-nickel alloys used in reactor internals. This is a complex subject covering a wide range of phenomena, (electrochemistry, physical metallurgy, mechanics, radiochemistry and irradiation damage), all of which interact to define the extent of general and localized corrosion (especially environmentally-assisted cracking (EAC)). A significant amount of research has been reviewed in this area for the ductile austenitic stainless steels [Ford et al, 2010] and nickel-base alloys [Scott et al, 2011], that are used in both PWRs and BWRs. This body of knowledge may be used as a guide to the expected degradation of the high-strength high-nickel alloys, since the compositions and many of the metallurgical and corrosion properties of these high-strength alloys are encompassed by those of the ductile austenitic alloys (Figure 3-1), (Table 3-1).

A tutorial is given in Appendix C that sums up the experience of degradation of Type 304 stainless steel and Alloy 600 used in the primary systems of PWRs and BWRs. Based on that background, it is expected that the following topics are of relevance to high-strength, high-nickel alloys (286, X-750, 718 and 625);

1) General corrosion.

The high strength, high-nickel alloys will have good general corrosion resistance in BWR and PWR primary environments of the order of a few tenths of a micron per year over extended operational times [Lister & McAlpine, 1984], [Robertson, 1991]. As explained in Appendix C the reason for this is understood in terms of the stability and low solubility of the surface oxides that protect the metal from the reactor coolant.

2) Accuracy of system definition and the relevance of accelerated test procedures.

The observed dependences of stress corrosion crack initiation and propagation on the various stress, environment and material parameters (Figure C-1) are very much a function of the accuracy in defining these parameters, and then monitoring and controlling them in laboratory tests. For example, the cracking sensitivity to changes in the electrochemical corrosion potential (ECP) can be high in certain potential ranges, and unless the ECP is monitored and controlled, this can lead to a large scatter in the observed data. Similarly accelerated tests are sometimes used in order to quickly obtain data. If this acceleration is achieved, however, by imposing complex stress patterns, applied strain rates, elevated temperatures, complex crevice geometries, etc. then the resultant conclusions may not be relevant to reactor operating conditions, especially if the rate limiting step in the degradation mechanism has changed.

3) Chronology of degradation events.

The chronology of events leading to “failure” of high-strength, high-nickel alloys due to environmentally-assisted cracking (Figure C-12) should follow the same general trend as those observed in ductile stainless steels and nickel-base alloys.

4) Dependency of crack initiation and propagation on stress (intensity factor).

Crack initiation on initially smooth surfaces of high-strength, high-nickel alloys will depend on tensile stress in much the same way as that on similar ductile alloys (Figure C-24). This dependency will be a function of the material heat treatment, environmental conditions, local strain concentrations due to surface cold work, etc.

Similarly the SCC crack propagation rate, V , as a function of the stress intensity factor, K , should follow the same general $A(K)^m$ dependency as observed in Alloy 600 and Type 304 stainless steel (Figure C-27). The values of “A” and “m” for BWR environments will be dependent on the combinations of ECP, grain boundary chromium depletion (sensitization) and anionic impurity concentration (Figure C-27 and Figure C-28). The dependencies for PWR primary environment will be different from BWR environments as will be discussed in Appendix C. Thus, the precise relationship for the effect of the stress (intensity factor) will, as mentioned above, be very much dependent on the monitoring and control of other system parameters. If that definition and control is not exercised then the V vs. K relationship will, as illustrated in Figure C-26, for Alloy 600 in PWR primary environments, exhibit a large amount of scatter.

- 5) Dependency of crack initiation and propagation on the electrochemical corrosion potential (ECP).

The crack propagation rate for the high-strength high-nickel base alloys should follow the same general ECP dependency as observed for the stainless steels (Figure C-31a) and ductile nickel-base alloys (Figure C-31b) in environments associated with BWR “normal water chemistry” and “hydrogen water chemistry”. The range in propagation rates for the ductile alloys is approximately 3 orders of magnitude for the ECP range from +200 mV_{she} in the reactor core, to -230 to -550 mV_{she} associated with “BWR-hydrogen water chemistry” or “noble metal technology”. Specific V vs. ECP relationships take into account differences in grain boundary sensitization, anionic impurity concentration and yield stress.

As will be discussed in Appendix C, the accelerated crack propagation rate for nickel-base alloys in the lower ECP range associated with PWR primary chemistries is restricted to a narrow potential range of approximately 100mV_{she} width around -800mV_{she}, with a maximum⁸ propagation rate a factor of x3 for Alloy 600, to x8 for Alloy 82 compared to the low background rates. This occurs when the dissolved H₂ concentration places the ECP value close to the Ni/NiO equilibrium potential (Figure C-35 and Figure C-37).

High-strength nickel-base alloys in PWR primary environments should follow the same dependency, and this is observed for Alloy X-750 (Figure C-36), similarly, unless there is a change in the cracking mechanism, the crack initiation time for the high-strength, high-nickel alloys should decrease with rising H₂ content in the PWR primary environment, as is seen with the ductile alloys (Figure C-35).

- 6) Effect of water purity.

The crack propagation rates for both stainless steels (Figure C-32) and ductile nickel-base (Figure C-33) alloys are sensitive to anionic impurities (especially chloride and sulphate) in more oxidizing environments associated with BWR “Normal Water Chemistry” conditions, and as the ECP lowers so this sensitivity decreases (Figure C-34). By extension, there should be a minimal effect of chloride or sulphate impurity concentrations under the low ECP conditions in BWR-HWC and PWR primary environments (Figure C-34).

There is no theoretical reason why these relationships should not be observed in the high-strength high-nickel base alloys used in BWRs and PWRs

⁸ Note that the lower Ni-content stainless steels do not exhibit this accelerated crack propagation rate and have exhibited a good performance in PWR-primary environments when there are no oxygen transients.

7) Effect of grain boundary composition and morphology.

Precipitation of Cr_{23}C_6 on the grain boundary of stainless steels and nickel-base alloys occurs in the temperature range 600-700°C (1112-1292°F) encountered during welding or stress relief heat-treatments. This topic has been reviewed elsewhere [Ford et al, 2010], [Scott et al, 2011] as well as in Section 3.4.1 in this report. The subsequent growth of the grain boundary carbides is accompanied by depletion of chromium in the adjacent matrix because of the slower diffusion rate of chromium compared with that of the carbon atoms. It is seen in Figure 3-21a that the chromium profile adjacent to the grain boundary in Alloy 600 is initially narrow and deep, but with longer times at temperature (in this case, 700°C), the Cr profile flattens out (“heals”) since there is time for the slower diffusing chromium atoms to migrate from the grain interior towards the growing grain boundary carbide.

Similar behaviour is observed in Alloy X-750 as illustrated in Figure 3-7b.

Of particular significance to the high-strength high-nickel alloys are the hardening heat treatments associated with γ' and γ'' precipitation (Table 3-4, Table 3-5, Table 3-7, Table 3-8 and Table 3-9) which may be in the range of 621-718°C for 10-80 hours. Thus Cr depletion at the grain boundaries in these alloys is to be expected, although healing at the longer aging times is likely.

It is open to debate as to which of the two phenomena, carbide precipitation on the grain boundary, or the associated Cr depletion in the adjacent grain matrix is of more relevance to SCC initiation and propagation.

In BWR environments under “normal water chemistry” conditions where the ECP is >-100 mV_{she}, intergranular attack and subsequent crack initiation are influenced by the chromium depletion at the grain boundaries. This chromium depletion also has an influence on crack propagation due to its effect on the passivation rate of the chromium-depleted grain boundary in the crack tip environment at the straining crack tip. As the corrosion potential decreases, however, to BWR “hydrogen water chemistry”, and ultimately PWR primary conditions, where the ECP < -230 mV_{she}, the effect on the crack propagation rate of the chromium depletion is very low.

On the other hand a high concentration of grain boundary carbides increases the PWSCC initiation time (Figure C-40) which was hypothesized by Angeliu et al. [Angeliu et al, 1992] to be due to increasing creep resistance occasioned by pinning of mobile dislocations in the grain boundary region.

In either case the SCC susceptibility of the high-strength, high-nickel alloys should have a similar sensitivity to the grain boundary structure as exhibited by the ductile alloys such as Alloy 600.

8) Effect of yield stress.

Increasing yield stress due to cold work, irradiation hardening, etc. is well recognized to increase the SCC propagation rate for stainless steels and ductile nickel-base alloys in LWR environments (Figure C-46 and Figure C-47). As will be discussed in Appendix C the effect may be understood in terms of increasing the strain rate in front of an advancing crack tip. Thus it is to be expected that the SCC susceptibility for the high-strength, high-nickel alloys, will be considerably enhanced compared with that observed in ductile stainless steels and nickel-base alloys with yield stresses circa 200 MPa, and that that increase will be more pronounced as the ECP is lowered (Figure C-48) and as the degree of grain boundary sensitization is decreased (Figure C-47).

Obviously this yield stress effect will be of significance when discussing the behaviour of the high-strength, high-nickel alloys.

6 Effects of composition on microstructure and properties (Alfred Strasser)

6.1 Effect of alloying elements

6.1.1 Nickel and niobium

The Ni and Nb contents determine the presence of the γ'' phase, body centred tetragonal Ni_3Nb , one of the hardening components of the precipitation hardening Alloys 718 and X-750. The control of this phase is significant for nuclear applications as discussed in Chapters 3 and 5. As discussed in those Chapters, the delta (δ) phase, the orthorhombic form of Ni_3Nb , can also form as a result of certain processing and heat treatment conditions. Alloys free of the delta phase are believed to be desired for high ductility, good fracture toughness, SCC resistant nuclear applications while a fine grain structure with fine dispersed delta phase is desired to obtain a creep resistant alloy for aerospace applications. The solvus temperature of Ni and Nb need to be known to establish effective heat treatments for obtaining these structures. The solvus temperature can be controlled by the Nb content, but the data on the effect of Ni on the solvus temperature by different investigators has not been in good agreement. In order to resolve this discrepancy, the effects of variations of Ni and Nb contents were evaluated within the specification range for Alloy 718, on the solvus, the microstructure and the mechanical properties [Frank et al, 2010].

Small vacuum melted ingots were prepared with three Ni levels (51.5%, 53%, 54.5%) and three Nb levels (5.0%, 5.2%, 5.4%), homogenized at 1120°C, hot forged and hot rolled starting at 1120°C. Samples were then treated at the solvus temperature range of 925°-1025°C in small increments. Consistent microstructures with a fine, ASTM 11-12 grain size, were observed in all cases. The Ni content had little or no effect on either the delta or the γ'' solvus temperature while the increase in Nb had the expected increase in both solvus temperatures (Figure 6-1).

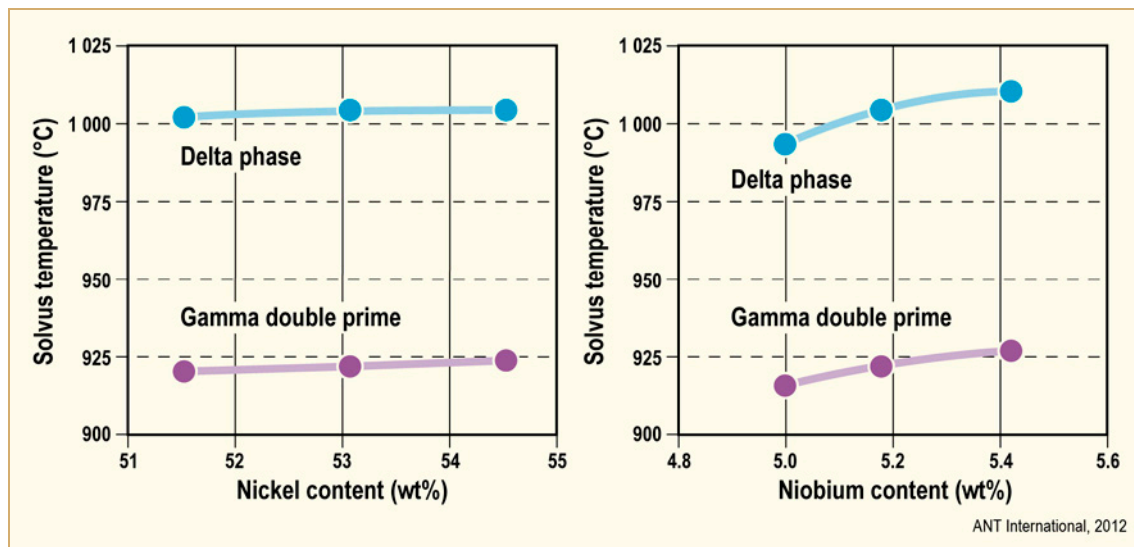


Figure 6-1: Effect of nickel and niobium contents on solvus temperatures of Alloy 718, after [Frank et al, 2010].

There was no significant effect of Ni content on the solution treatment related hardness, but recrystallization temperature and hardness increased for the higher Nb levels (Figure 6-2).

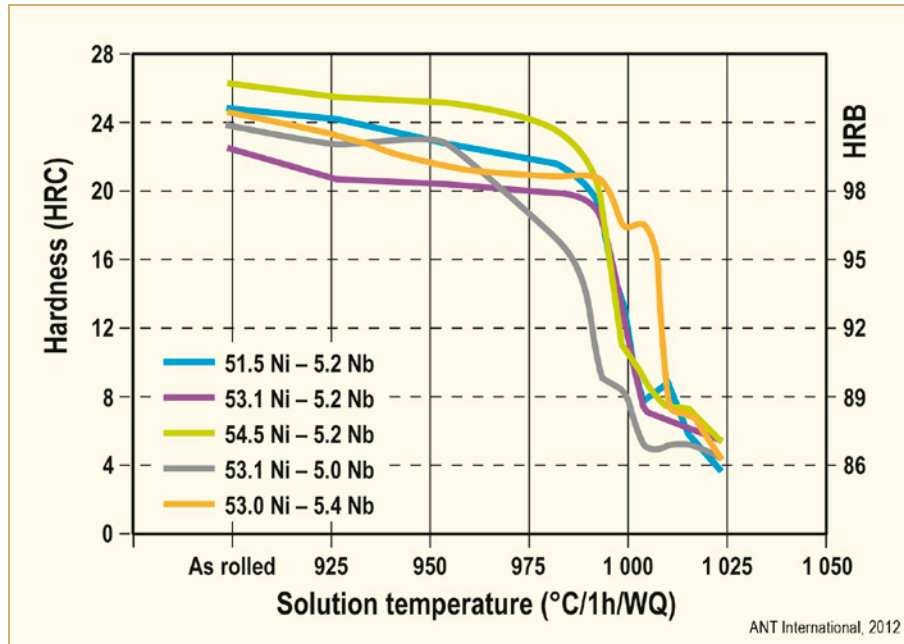


Figure 6-2: Effect of solution treatment temperature on hardness of Alloy 718 with variations in nickel and niobium contents, after [Frank et al, 2010].

The effect on mechanical properties was tested after exposure of two different heat treatments optimized for,

aerospace applications: 954°C/1 hr/AC + 718°C/8 hr/FC to 621°C/8 hr/AC

oil-field applications: 1024°C/1 hr/OQ + 785°C/6 hr/AC

The variations in Ni content had no significant effect on room temperature tensile, stress-rupture or impact properties for either heat treatment. The higher Nb content range increased strength and reduced toughness. The oil-field heat treatment produced 3-5 times higher toughness compared to the aerospace treatment partly due to lower strength and higher ductility and partly due to the absence of the delta phase. However the delta phase is essential for creep rupture notch ductility at elevated temperatures, but can reduce impact, fracture toughness and SCC resistance at lower temperatures.

6.1.2 Carbon and chromium

Japanese investigators evaluated the effect of varying amounts of carbide formers such as carbon (C), chromium (Cr) and molybdenum (Mo) on SCC, in alloys similar to Alloy X-750 and Alloy 718 [Yonezawa et al, 1986]. The specimens tested were vacuum induction melted and heat treated under different conditions. The SCC specimens were U-bend samples tested in a loop simulating PWR coolant conditions at 360°C.

The results for a material similar to Alloy X-750 are shown on Figure 6-3 and for a material similar to, but modified Alloy 718 are shown on Figure 6-4. The differences in heat treatment did not have a significant effect on SCC but had some effect on tensile properties at room temperature and 360°C, compared to the variations in alloying comment. *Increased C and Cr contents indicate increased SCC resistance; however, since these data were not related to a microstructure in the publication (only the Abstract and slides are available), the application of these trends should be limited to these compositions and heat treatments.*

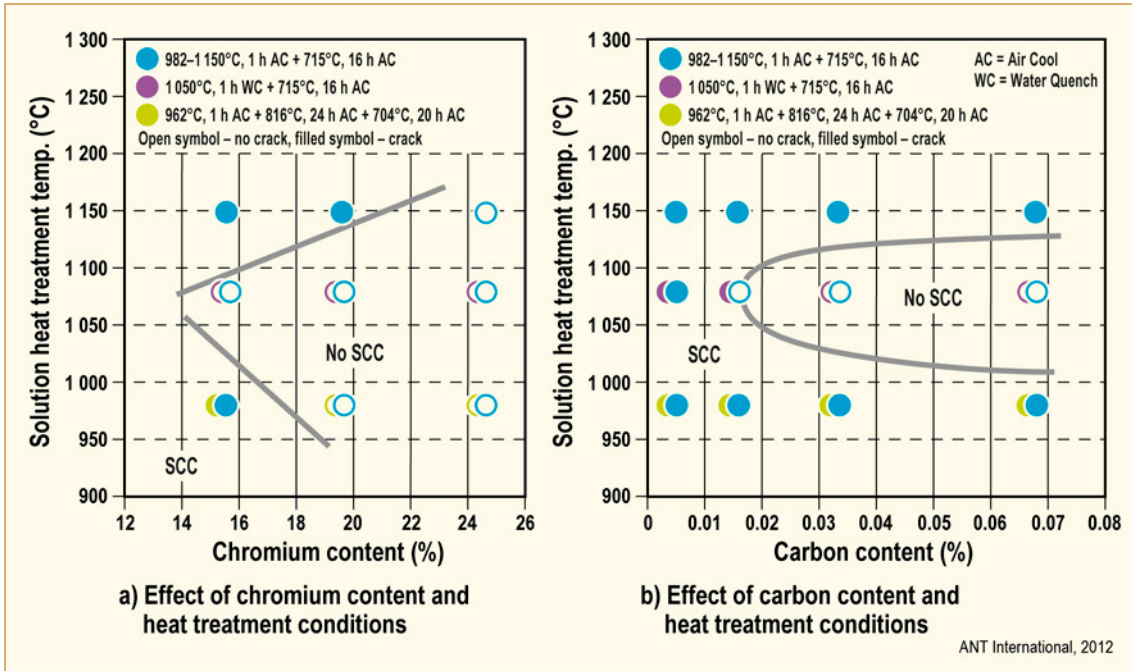


Figure 6-3: Effect of carbon and chromium contents on SCC of a Ni base alloy of 15% Cr - 7% Fe - 2.5% Ti - 1% Nb - 0.7% Al (Similar to X-750), after [Yonezawa et al, 1986].

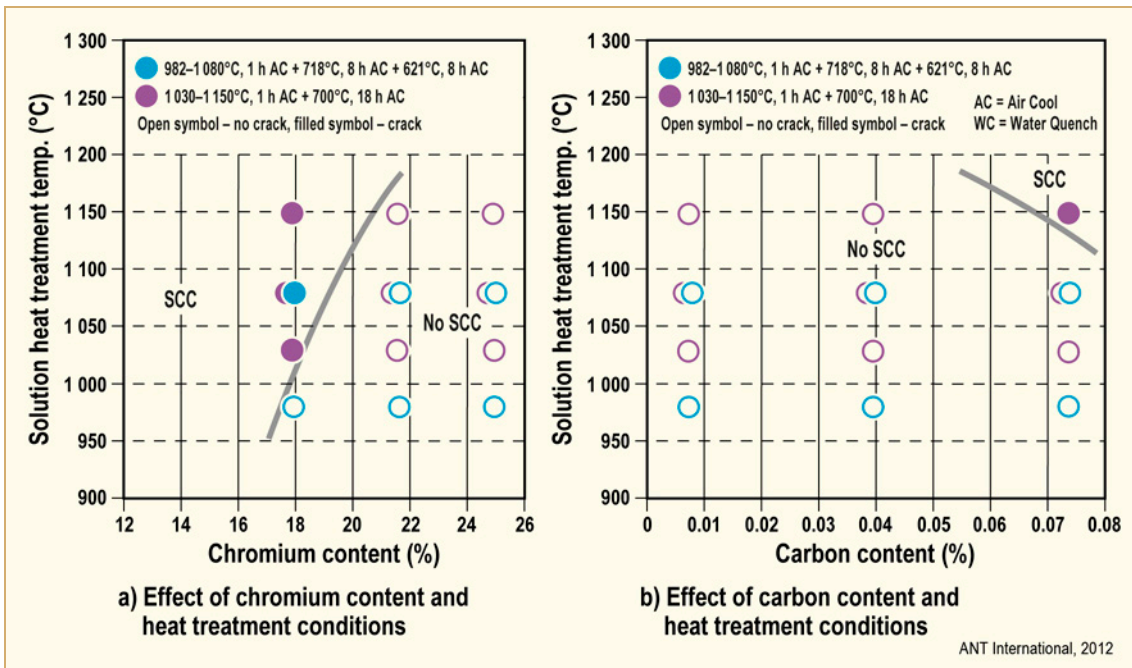


Figure 6-4: Effect of carbon and chromium contents on SCC of a Ni base alloy of 22% Cr - 16% Fe - 3% Mo - 6% Nb - 0.4% Al - 0.1% Ti (Similar to 718), after [Yonezawa et al, 1986].

7 Effects of irradiation on microstructure and properties (Alfred Strasser)

7.1 Introduction

When metals are irradiated by neutrons, or by charged particles such as protons, electrons or ions, their energy is dissipated in the crystalline structure of the metals and the process affects the structure and properties of the metals in a variety of ways that include:

- Modification or change in the crystal structure,
- Modification or change in the secondary phases, their composition, size and distribution, and its effects on the composition of the matrix phase,
- Transmutation of elements into new isotopes and chemical elements,
- Segregation of elements in grain boundaries,

These changes in the structure of the metals can result in changes to the mechanical properties, physical properties, physical dimensions, and resistance to corrosion, including stress corrosion cracking (SCC). The changes resulting from irradiation are discussed in the subsections to follow, with the exception to the irradiation assisted stress corrosion cracking (IASCC), which is discussed in Chapter 5.

7.2 Crystal structure

Metals have a crystalline structure made of a well-defined, precise array of atoms. However, the crystalline structures have defects in these arrays which have a significant effect on the metal properties and on their deformation mechanisms under stress. These are in the form of point defects, vacancies and interstitials and are present in metals when they are at their equilibrium; they are illustrated in Figure 7-1. A *vacancy* is the absence of an atom at a normally occupied lattice site and an *interstitial* is in a position between normal lattice sites, a “self” interstitial if of the same material and “impurity” interstitial if it is a different material.

Dislocations are lines that form a boundary between a region of the crystal that has or has not been deformed. They are defects that are intrinsic to a crystal, and their numbers can be increased by external forces, such as cold working. They can also be formed as a dislocation loop when a sufficient number of vacancies and interstitials condense on a particular plane. The dislocations act as both a source and a sink for point defects and as such, attract interstitials and vacancies as well. A grain boundary is still another defect that exists at the interface of two crystals of different orientations. This is an important area whose characteristics can modify many of the metal properties.

The energy of neutrons, and of charged particles, is dissipated when they collide with the atoms of a solid crystal in an either elastic or inelastic collision. In an elastic collision the neutron transfers its energy to the nucleus and its direction of motion is deviated. The first atom to be hit will be ejected from its equilibrium position if the energy is sufficient to create a vacancy, and can stop at an interstitial position, generate other displacements or create a cascade of atom displacements that consist of vacancies and interstitials. The vacancy and interstitial loops can form in the process. The dislocation loop microstructure will harden the material and react elastically with the dislocation network under an applied stress to increase the yield and tensile strength. The modified crystal structure will also alter the deformation process of the material significantly and affect its mechanical properties as discussed in Section 7.3.

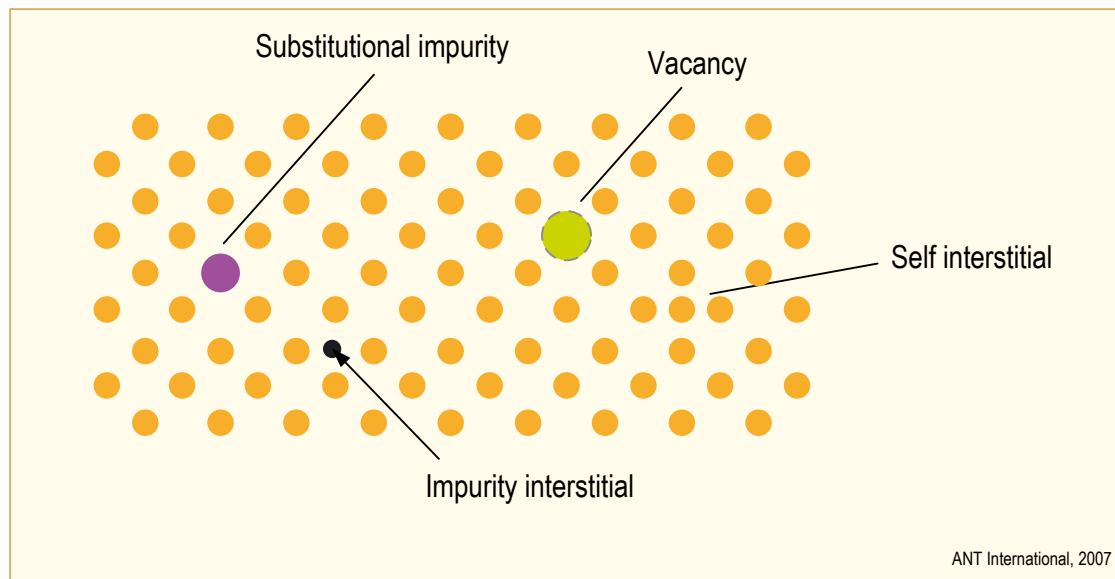


Figure 7-1: Four types of point defects, after [Dowling, 1999].

In an inelastic collision the neutron can be absorbed by the nucleus which in an excited state gives off γ radiation and a neutron ($n, n'\gamma$ reaction), but no defects are created by this process in the crystal structure. However, some elements can absorb neutrons and cause different reactions that lead to the formation of chemically different atoms, a process called transmutation. Prime examples are (n, α) and (n, p) reactions that produce helium and hydrogen respectively and have a significant effect on the properties of the material as discussed in Section 7.4.

Detailed descriptions of the effects of radiation on the crystal structure are given in two ANT International Special Topical Reports, “Impact of Irradiation on Material Performance” [Adamson & Cox, 2005/2006] and “In-Reactor Creep of Zirconium Alloys” [Adamson et al, 2009].

7.3 Microstructure and mechanical properties

7.3.1 Introduction

Irradiation has a significant effect on the complex microstructure and properties of Ni alloys. While there is an extensive literature on the effect of irradiation on Ni alloy properties in the stainless steel category of 8%-15% Ni, the data on alloys >25% Ni are more limited. It should be noted that these alloys have either a body centred or face centred crystal structure (BCC or FCC), unlike zirconium alloys which have a hexagonal closed packed structure (HCP)

Experimental data on the high strength Ni alloys are summarized by alloy in this section. Irradiated properties related to the IA SCC of the high Ni content alloys are discussed in Chapter 5. The transmutation of ^{59}Ni to He and H has a significant effect on creep properties and that effect is discussed in Section 7.4.2 on Transmutations. The data related to actual components exposed in reactors are summarized in Chapter 8.

7.3.2 Alloy 718

Microstructure

Two heats of Alloy 718 of slightly different composition (Table 7-1) were irradiated in a PWR at 288°C to exposures of 2.5 dpa (heat c) and 3.5 and 20 dpa (heat d), assuming 1 dpa to be equivalent to 0.7×10^{21} n/cm² (E>1 MeV). Both heats were heat treated at 954°C/1 hr + 718°C/8 hr + fc to 621°C/8 hr. The changes in microstructure and hardness were compared to the unirradiated archive samples [Thomas & Bruemmer, 1997].

Table 7-1: Chemical composition of Alloy 718 heats, wt%, after [Thomas & Bruemmer, 1997].

Heat	C	Fe	Ni	Cr	Mn	Mo	Nb	Ti	Al	Si	N	S	P	Cu	B	Co
c	0.06	19.2	52.0	18.1	0.2	3.1	5.3	1.0	0.6	0.23	0.007	0.001	0.015	0.10	0.006	0.24
d	0.03	19.6	52.7	18.0	0.0	3.0	5.1	1.0	0.6	0.06	0.005	0.002	0.026	0.08	0.006	0.01

ANT International, 2012

The compositions of the precipitates in the unirradiated condition are given in Table 7-2. The second phase particles included γ' , γ'' , δ , carbides, Laves phase (heat c), G phase (heat d). Examinations of the irradiated samples indicated instabilities of the hardening phases, γ' and γ'' , and micro-chemical changes in the grain boundary. The original γ'' particles disappeared completely after 3 dpa and were only faintly visible after 2.5 dpa. The γ' phase dissolved slowly in the matrix and then started to re-precipitate in smaller particles in the matrix at the lower dose and after 20 dpa all the original 10 nm particles were replaced by 1 nm particles dispersed in the matrix, exclusive of grain boundaries and dislocations. The progression of the microstructure as a function of exposure is shown on Figure 7-2.

Table 7-2: Precipitate compositions in Alloy 718 measured by TEM-EDS, wt%, after [Thomas & Bruemmer, 1997].

Phase	Al	Si	Ti	Cr	Fe	Ni	Nb	Mo	Compound
δ	0.2	0.2	2.2	2.1	3.8	61.4	29.6	0.5	Ni ₃ (Ti, Al Nb)
Laves	0.2	2.6	0.3	12.1	12.4	30.1	28.6	13.8	
γ''	0.1	0.4	1.9	2.9	3.6	64.9	24.2	2	Ni ₃ Nb
NbC	0	0.2	7.9	1.7	1.5	3.4	91.9	0	
TiC	0.1	0.1	64.6	0.9	0.9	1.6	31.4	0.4	
G	1	15.9	1.6	3.7	6.3	50.1	21.4	0	

ANT International, 2012

8 In-reactor performance of high nickel alloy fuel assembly components (Alfred Strasser)

8.1 Introduction

The performance of fuel assembly components made of high Ni alloys is summarized in this section with emphasis on failures and their potential remedies. Included in the summary are Alloys 600, 625, 718, X-750 and A286.

The majority of the applicable literature was published in the mid-1980s or before. The performance problems of these alloys since then have either been reduced or are not published. A good summary of the early failures is given by [Miglin et al, 1986] in Table 8-1.

Initially Alloy X-750 and to a lesser extent A286 were the most frequently used high Ni alloys used for components requiring high strength. Performance problems brought Alloy 718 to compete with Alloy X-750, while the use of A286 was essentially stopped. The two precipitations hardened Alloys 718 and X-750 are currently the most frequently used, each with its own limitations discussed in previous sections.

The solution strengthened Alloy 625 has been used successfully where somewhat lower stress levels are permissible.

The best choice between Alloy 718 and X-750 for either PWR or BWR applications has still not been resolved. A comparison to help resolve their use for PWRs was made by evaluating their IGSCC resistance in a PWR environment. The slow strain rate tensile tests (SSRT) concluded that although there are some secondary disparities in behaviour, both alloys present a similar susceptibility to environmental damage and to crack initiation [Ter-Ovanesian et al, 2009].

Details of this test are discussed in Chapter 5. In general, Alloy 718 would be preferred for the more highly stressed applications.

The choice for BWRs by GNF and Westinghouse for spacers and other structural components has been Alloy X-750; however, the Japanese vendors favour Alloy 718 for spacers for its higher strength and the claim that Alloy X-750 is subject to crevice corrosion and may be less resistant to crack initiation. The current, as yet unannounced, operation of some BWR assemblies with Alloy 718 spacers would not be surprising.

Continued failures occur with both Alloy 718 and X-750 in spite of the successful performance of thousands of components made from these alloys. While the application of lower strength Alloy 625 in fuel assemblies is much more limited than the higher strength Alloy 718 and X-750, the absence of any failure reports for this material would make it a candidate for further investigation in its annealed, cold worked or even aged condition. Alloy 725, and advanced precipitation hardening version of Alloy 625, has not been used for nuclear applications at the time of this report.

Table 8-1: Examples of the reactor internal component failure histories of age-hardenable, high strength Ni-base alloy [Miglin et al, 1986]. Reproduced from [Hanninen & Aho-Mantila, 1987].

Component	Heat Treatment	Environment	Remarks
Alloy X-750			
Fuel assembly hold-down springs (B&W)	No. 1 temper; Hot rolled and sol. Anneal at 1149°C plus 15% cold work plus 732°C/16 h	316°C PWR primary coolant	1% failure rate; most failures from one heat with microstructural anomaly (HT72F7XS); mixed fatigue and IGSCC
Baffle-to-former bolts (KWU)	927°C anneal; 729°C/8 h; 621°C/8 h	343°C PWR primary coolant	10% failure rate in 4 years of service, high (690 to 1380 MPa) bending stress UGSCC,
Fuel assembly bolts (ASEA-ATOM)	Unavailable	BWR coolant	High static service stress; IGSCC
Control-rod-drive guide tube support pins (Westinghouse, France, Japan)	Various heat treatments 1149°C/0.5-24 h 621-843°C/8-20 h	299/327°C PWR primary coolant	High (890 MPa) bending stress, IGSCC
Jet pump beams (GE, foreign BWR's)	Hot rolled plus 885°C/24 h plus 704°C/20 h	BWR coolant	Highly stressed; IGSCC
Alloy 718			
Fuel assembly hold-down spring (B&W)	Hot roll; 1038° anneal; cold drawn; 982°C anneal; cold drawn, coiled; 768°C/ 8 h; 621°C/10 h	316°C PWR primary coolant	1 failure out of 150 springs; 455 MPa max torsional service stress; fatigue initiated by fretting
Barrel-design hold-down springs (Westinghouse)	Annealed; cold drawn, coiled, 718°C/8 h; 621°C/10 h	316°C PWR primary coolant	12% failure rate; fatigue
Alloy A 286			
Reactor vessel internals bolting (B&W)	ASTM A 453, Gr. 660, Cond. A and B	PWR primary coolant	0.5% to > 50% failure rate, depending on application; IGSCC
Guide bar bolts; cover beams (ASEA-ATOM)	920°C/1 h; 720°C/16 h	BWR coolant; steam	30% failure rate for guide bar bolts; high stresses; IGSCC

ANT International, 2012

The majority of the failures have been ascribed to a combination of excessive stresses and non-optimal heat treatments and microstructures that cause stress corrosion cracking (SCC) or irradiation assisted SCC (IASCC). Fatigue has also been a failure cause in some applications. Inadequate specifications and qualification of fabrication processes appear to contribute to failure causes as well.

The potential effects of He voids produced by ^{10}B transmutation had been recognized in a few cases and a <10 ppm B level has been recommended as a result. No examination results have been published of the more recently identified, potentially significant effects of thermal neutron induced ^{59}Ni transmutation to He and H on microstructure, properties and performance in LWRs. Extensive literature exists on the fast neutron induced transmutations in stainless steels and high Ni alloys for fast breeder applications at 650-750°C compared to 300-350°C for LWRs. Since both the mechanism of damage and temperatures are different from the LWRs, the data are not included in this section.

8.2 Spacer grids

8.2.1 PWRs

A relatively recent design modification of the Westinghouse assemblies consists of an additional grid made of Alloy 718, located above the lower nozzle, called a Protective Grid (P-grid), whose function is to limit flow induced vibration of the fuel rods and act as a debris filter as well. The dimples on the P-grid and occasionally some ligaments have cracked without producing debris; however, as the failures progressed cracked dimple pieces have turned into debris and caused fuel failures in a number of plants. Westinghouse analysis showed that the cause of the failures was hydraulic force induced strap vibration resulting in fatigue cracks (Figure 8-1). The remedy has been a redesigned grid with modified structure and flow holes to minimize the hydraulic effects [Evans et al, 2011].

The mechanism driving the strap vibrations was determined to be vortex shedding off the grid strap edges and the re-design effort was aimed at disrupting this process. The vibration frequency can be as high as 3600 Hz at normal 4.6 m/s flow rates. If the vortex shedding frequency off the grid strap is near the natural frequency of the grid strap, “lock-in resonant vibration” occurs and leads to unacceptable high frequency vibration. Vibration analyses and loop tests led to a series of improved designs from the original vibration prone one in Figure 8-2a, to an improved one in Figure 8-2b by eliminating a horizontal vibration promoting ledge. Cut-outs of various shapes on the top and bottom edges were found to promote vibration reduction further and led to the design, as published, in Figure 8-2c, a part of the new design called the Robust Protective Grid (RPG). A 500 hour loop test of the RPG showed zero failures compared to 75 fatigue failures per grid of the original design.

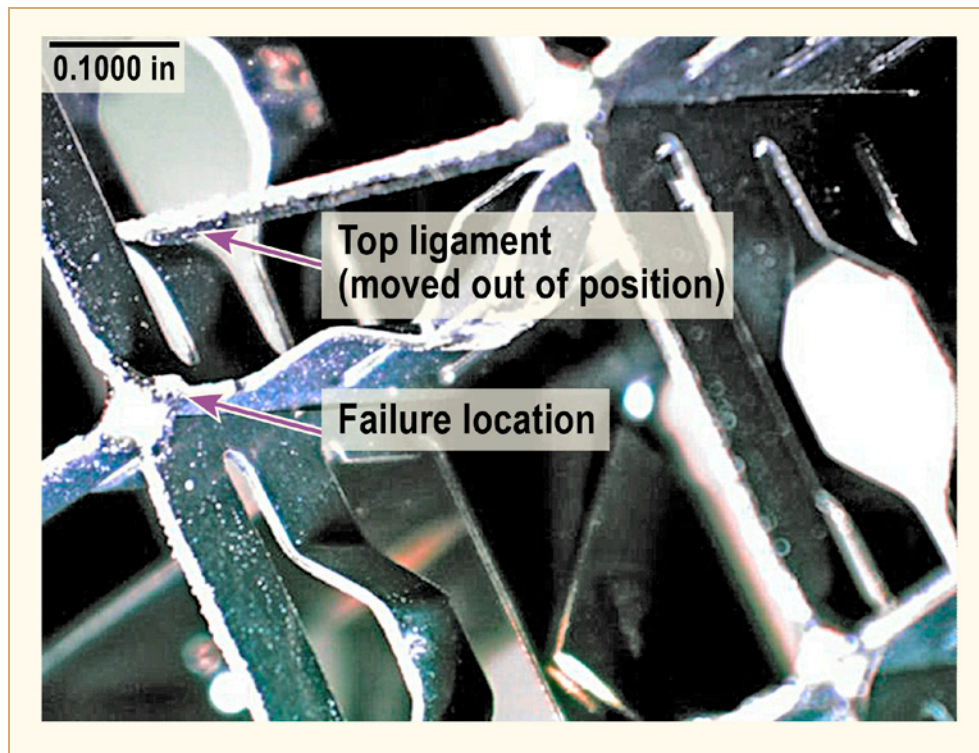


Figure 8-1: Alloy 718 protective grid fatigue failure [Evans et al, 2011].

9 Conclusions relevant to LWRs

9.1 Applications (Alfred Strasser)

- The high strength Ni alloys that currently form a part of the fuel assembly structures are Alloys 718, X-750 and 625 and have been adopted by all Western fuel vendors. They have generally performed well, with intermittent failures of Alloys 718 and X-750 starting in their application in the initial LWR designs continuing to some of the current designs.

9.2 Unirradiated physical and mechanical properties (Alfred Strasser)

- The alloys have excellent tensile and creep-rupture properties, good ductility and excellent oxidation resistance up to high temperatures well above those in LWRs.
- The creep strength and endurance limits can be improved significantly by small grain size microstructure of about ASTM 8 or higher.
- The properties are highly sensitive to heat treatments and irradiation effects noted in conclusions that follow.

9.3 Physical metallurgy of unirradiated alloys (Peter Ford)

- The development of high-strength, high-nickel alloys for application in LWRs has its origin in the use of such “superalloys” in gas turbines and aircraft engines operating at temperatures >650°C. The required properties for these very high temperature applications are high temperature strength, and resistance to (dry) oxidation, fatigue and creep. These requirements are not necessarily relevant to LWR irradiated aqueous environments, although some have some bearing; for instance, the mechanisms for increasing strength are common to both applications, as is the need for resisting creep (since time dependent plasticity at the crack tip is a common feature for various SCC mechanisms).
- The strengthening mechanisms relevant to the targeted high-strength alloys (X-750, 718, 625 and 286) are precipitation hardening, solid solution hardening, work hardening and grain refinement. Precipitation hardening is the dominant mechanism, although components of the other strengthening mechanisms have a role depending on the specific alloy.
- Precipitation hardening of Alloys 286, X-750 and 718 is associated with the precipitation of the face centred cubic γ' ($\text{Ni}_3(\text{Al,Ti})$) phase, with the extent of the strengthening depending on the size and volume of the γ' in the austenitic grain matrix. The precipitation hardening of Alloy 718 is supplemented by additional precipitation of the body centred tetragonal γ'' (Ni_3Nb) phase, which may also supplement the solid solution hardening of Alloy 625.
- For these precipitation hardening procedures to be successful it is necessary to solution anneal the alloy in a high enough temperature range (e.g. 1037 to 1065°C (1900-1950°F)) in order to take all of the γ' and γ'' into solution and then age in the range 621°-704°C (1150-1300°F) for 18-80 hours (depending on the alloy) in order to precipitate a uniform dispersion of γ' and γ'' nanoparticles in the grain matrix.

- Intermediate aging treatments involving temperatures in the range 704-843°C (1300-1550°F) have been, in the past, inserted between the solution annealing and precipitation hardening aging treatments. This was done in order to “stabilize” the grain structure by carbide precipitation and thereby improve the stress rupture and creep properties of superalloys operating at gas turbine operating temperatures. Such “stabilization” heat treatments lead, however, to diminished SCC resistance in both PWR and BWR primary environments. Consequently such heat treatments are no longer recommended and reliance is centred on using elevated solution heat treatments in order to ensure that the γ' and γ'' phases are taken into solution before applying a “direct age”.
- The γ' and γ'' phases are metastable at elevated aging temperatures and transform to the hexagonally close packed η (Ni_3Ti) and orthorhombic δ , Ni_3Nb phases respectively. These η and δ phases do not contribute to precipitation hardening because of their size and lack of coherency between their atomic structures and that of the γ matrix. These phases can be beneficial when on the grain boundary in restricted amounts, since they can inhibit excessive grain growth. However they can also be deleterious to mechanical properties due to their brittle nature and acicular morphology.
- Precipitation of η and δ phases on the grain boundaries can lead to γ' and γ'' free zones where localized plasticity can then occur leading to a potential increase in the SCC susceptibility and grain boundary embrittlement.
- Primary carbides such as NbC, TiC, can also be effective grain size refiners, but there is the danger of uneven grain sizes if the carbides are unevenly distributed during casting and rolling operations. This macroscopic heterogeneity can lead to orientation effects (“banding”) on stress corrosion crack initiation and propagation.
- Carbides may also be in the form of chromium-rich M_{23}C_6 particles precipitated on the grain boundary during the γ' and γ'' aging treatments. Such carbide precipitation can lead to Cr-depletion in the γ matrix adjacent to the M_{23}C_6 , and this may have a deleterious effect on the SCC resistance in some LWR environments.

9.4 Fabrication of alloys (Alfred Strasser)

- The alloys are vacuum melted, re-melted by a consumable electrode process and potentially re-melted by a variety of additional processes in order to obtain good alloy and structural homogeneity, remove oxygen, nitrogen and hydrogen as well as evaporate undesirable trace elements. Vacuum induction melting (VIM) followed by vacuum arc melting (VAR) is the most common sequence for nuclear applications.
- Impurity control is very important. Two of the most damaging impurities are sulphur (S) which affects properties and hot workability and bismuth (Bi) which can reduce creep ductility and affect hot workability as well.
- Cobalt (Co) levels need to be kept low to minimize activity transport by the coolant. A level well below 0.1% is desirable and deliverable on special order, however, may not be available since Alloy 718 made primarily for aerospace applications maintains the Co level “as-is” which can be 0.5% to 1.0%.
- Boron transmutes to helium and lithium under irradiation with detrimental effects on properties and for nuclear applications should be kept at <10 ppm which can be obtained, however, B is actually added for aerospace applications for improvement of their properties.
- The control of alloy and grain size homogeneity is important. Longer holding times and magnetic stirring of the pool improve homogeneity and reproducibility of the products.

10 References

- Adamson R. B. and Cox B., *Impact of Irradiation on Material Performance*, ZIRAT10/IZNA5 Special Topics Report, ANT International, Mölnlycke, Sweden, 2005/2006.
- Adamson R. B., Garzarolli F. and Patterson C., *In-Reactor Creep of Zirconium Alloys*, ZIRAT14/IZNA9 Special Topical Report, ANT International, Mölnlycke, Sweden, 2009.
- Andresen P. L., Emigh P. W., Morra M. M. and Horn R. M., *Alloy X-750 Stress Corrosion Crack Growth Rate Behaviour In High Temperature Water*, Proceedings of Eleventh International Conference on Environmental Degradation in Nuclear Power Systems–Water Reactors, Skamania Lodge, Eds. G. Was, L. Nelson, American Nuclear Society, pp. 787-804, August 5-9, 2003.
- Andresen P. L., Emigh P. W., Morra M. M. and Horn R. M., *SCC of High Strength Ni-Base Alloys in High Temperature Water*, Corrosion-2004, Paper 04675, published by NACE International, 2004.
- Andresen P., Flores-Preciado J., Morra M. and Carter R., *Microstructure and SCC of Alloy X-750*, 15th Symposium on the Environmental Degradation of Materials in Nuclear Power Systems – Water Reactors, Virginia Beach, Virginia, August, 2009.
- Andresen P. L., Flores-Preciado, Morra M. and Carter R., *Microstructure and SCC of Alloy X-750*, Proceedings of Fifteenth International Symposium on Environmental Degradation in Nuclear Power Systems–Water Reactors, Colorado Springs, Eds. Busby J, Ilevbare G. and Andresen P. L. The Metallurgical Society, pp. 719-740, August 1-5, 2011.
- Angeliu T. M., Sung J. K. and Was G. S., *The Role of Carbon and Chromium on the Mechanical and Oxidation Behaviour of Nickel-base Alloys in High Temperature Water*, in “Proceedings of 5th Symposium on Degradation of Materials in Nuclear Power Systems”, Pub. NACE, Monterey Ca, pp. 475-479, 1992.
- Bajaj R., Mills W. J., Lebo M. R., Hyatt B. Z. and Burke M. G., *Irradiation Assisted Stress Corrosion Cracking of HTH Alloy X-750 and Alloy 625*, 7th Symposium on the Environmental Degradation of Materials in Nuclear Power Systems – Water Reactors, Breckenridge, Colorado, NACE, August, 1995.
- Bajaj R., Mills W., Kammenzind B. and Burke M., *Effects of Neutron Irradiation on Nickel-Base Fastener Alloys*, 9th Symposium on the Environmental Degradation of Materials in Nuclear Power Systems - Water Reactors, Newport Beach, California, NACE, 1999b.
- Baty D., Hayner G., Clevinger G. and Garner G., *Metallurgical Factors Affecting the Failure of Alloy X-750 Holddown Springs*, 1st Symposium on the Environmental Degradation of Materials in Nuclear Power Systems, Myrtle Beach, South Carolina, August, 1983.
- Bengtsson B. and Korhonen S., *Behaviour of A286 in BWR environments; Service Experience and Test Results*, in Proceedings of First International Symposium on Environmental Degradation in Nuclear Power Systems – Water Reactors, Myrtle Beach, August 22-25, 1983. Eds. J. Roberts, W. Berry, National Association of Corrosion Engineers, pp. 179-191, 1983.
- Bengtsson B., Dahlbaeck M., Jansson C. and Morin U., *Constant Load Tests of Age-Hardened Nickel Based Alloys in Oskarshamn 2 BWR*, EPRI RP-2181-1 and EPRI NP-6363, September, 1986.
- Benhamou C., Daret J. and Van Duysen J.C., *Contribution of Laboratory Studies to the Understanding and Solution of Tube Guide Pin Cracking Occurrence*, Contribution of Materials Investigation to the Resolution of Problems Encountered in Pressurized Water Reactor Plants: Proceedings of the International Symposium Fontevraud II, SFEN, Paris, September 10-14, 1990.

- Benhamou C. and Amzallag C., *Influence of manufacturing parameters on stress corrosion cracking of Alloy 600 used in nuclear power plants*, Proceedings of Eurocorr '99, 1999.
- Benhamou C., Chambrin J. L., Todeschini P., Champredonde J. and Lemaire E., *Evolution de la conception, de la fabrication et du montage des broches de fixation des tubes guides de grappes en Alliage X750*, Proceedings Convention Nationale SFEN, 2004.
- Bertram L. et al, *The Macroscale Simulation of Remelting Processes*, JOM, vol. 50, No. 3, pages 18-21, 1998.
- Betteridge W. and Franklin A. W., J Inst. Metals, Vol. 85, pp. 473-479, 1956.
- Bieber C. G. and Radebaugh R. J., in *Precipitation from Solid Solutions*, p. 417, ASM, Cleveland, Ohio, 1959.
- Boehlert C., Dickmann D. and Eisinger N., *The Effect of Sheet Processing on the Microstructure, Tensile, and Creep Behaviour of INCONEL Alloy 718*, Metallurgical and Materials Transactions, Volume 37A, Page 27, January, 2006.
- Boothby R., Journal of Nuclear Materials, Vol. 230, pages 148-157, 1996.
- Boothby R., *Radiation Effects in Nickel Base Alloys*, Volume 4, Comprehensive Nuclear Materials, Elsevier, Amsterdam, 2012.
- Broomfield G., *Irradiation Effects in Structural Alloys for Thermal and Fast Reactors*, pages 38-66, ASTM STP 457, 1965.
- Brucelle O., *Etude de L'effet de la microstructure sur la resistance a la corrosion sous contrainte en milieu primaire REP de alliage 718*, PhD Thesis, University of Toulouse, 2001.
- Burke M., Majer T. R. and Wilson I. L. W., *The Effect of Cooling Rate on Precipitate Morphology in Alloy X-750*, Proceedings of Fifth International Symposium on Environmental Degradation in Nuclear Power Systems–Water Reactors, Monterey, Eds. D. Cubicciotti, E. Simonen, American Nuclear Society, pp. 287-293, August 25-29, 1991.
- Burke M. G., Mager T. R. and Nelson J. L., *Stress Corrosion Cracking of Chemistry Variants of Alloy 718 Part 2 Microstructural Characterization*, Proceedings of Sixth International Symposium on Environmental Degradation in Nuclear Power Systems–Water Reactors, San Diego, Eds. E Simonen, R. Gold, National Association of Corrosion Engineers, pp. 821-827, August 1-5, 1993.
- Burke M. B., *Microstructural Characterization of Alloy 718*, EPRI Report TR-103970, Sept. 1994.
- Byun T. and Farrell K., *Tensile Properties of Inconel 718 After Low Temperature Neutron Irradiation*, Journal of Nuclear Materials, Vol. 318, pages 292-299, 2003.
- Carnahan R. A and Gordon G. M., *Progress on EPRI contract NP6362*, 1989. (Cited by [Pathania, 2002]).
- Causey A., Carpenter C. and MacEwen S., *In-Reactor Stress Relaxation of Selected Metals and Alloys at Low Temperatures*, Journal of Nuclear Materials, vol. 90, pages 216-223, 1980.
- Carpenter Technology Corp., *An Introduction to Premium Melting*, June, 2009.
- Chaouadi R., Scibetta M., Van Nieuwenhove R., Smolders B., Weber M. and Willekens M., *Irradiation Creep Inducing Stress Relaxation of Precipitation Hardened Inconel 718 Exposed to 0.5 dpa at 300°C*, SCK.CEN, BLG-843, April, 2000.

Appendix A – History of nickel alloy development and the rationale for their choice in LWR applications (Peter Ford)

The materials of construction for the primary circuits in LWRs were originally selected based on experience from the nuclear navy, and the aerospace and chemical industries.

A major design criterion, at least for the US reactors, (where most of the early designs of BWRs and PWRs originated), was adherence to the American Society of Mechanical Engineers [ASME, 1969] Section III code¹⁵ which, in 1977, concentrated on mechanical properties¹⁶. There was no code-requirement to take into account the effect of the reactor environment on, for example, fracture toughness, or the propagation of cracks due to Stress Corrosion Cracking (SCC)¹⁷. Indeed, the 1977 ASME III code stated that “*Protection against environmental effects, such as corrosion and radiation effects, is the responsibility of the designer*”. Consequently, given the number of reactor manufacturers, there has been a wide variety of alloys and heat treatments deployed for specific applications, with the final choice of alloy being a function of economics and a compromise depending on the alloy response to different degradation modes.

Nickel-base alloys have been an attractive choice for materials of construction in LWRs based on their satisfactory use in other industries over many years. These alloys have been developed since the early 1900's because of both their high ductility and fracture resistance, and their high corrosion resistance over a wide range of acidic and alkaline environments. This latter attribute is due, as discussed in Chapter 5, to the stability of nickel in water in reducing environments, and the presence of various low solubility oxide surface films in more oxidizing environments.

In addition to these basic mechanical and electrochemical attributes, nickel is able to hold in solid solution significant amounts of various alloying elements (Cu, Cr, Mo, Fe, W), thereby opening up the development of solid solution strengthened alloys with enhanced corrosion resistance in a number of challenging environments. Other alloying elements, such as Ti, Al and/or Nb may confer strengthening via precipitation hardening.

A discussion of the development of the various high-strength, high-nickel alloys used in water cooled reactors starts with commercially pure nickel (Alloy 200). The initial alloying element addition was copper leading to the nickel-copper alloy, Monel™ (Alloy 400) in 1906; this was prompted by the similarity between the composition of the alloy (Ni-30%Cu) and the “matte” produced during the extraction process from the ore. This alloy, Monel™, exhibited excellent corrosion resistance in seawater and more aggressive environments such as fluoride salts used in UO₂ processing, and was widely used in high pressure feed water heaters for fossil fired power stations. The addition of Al and Ti (typically 2.3-3.15% Al and 0.35-0.85% Ti) imparted a marked increase in strength due to precipitation hardening, and the resultant commercial alloy K-Monel™ (Alloy K500) has found use in marine environments for fasteners, propeller shafts, etc.. However, apart from some isolated use early on in feed water heaters for water cooled nuclear reactors, its use in primary coolant environments has not been widespread due to the danger of copper contamination and ensuing Crud-Induced Localized Corrosion (CILC) of zirconium alloy fuel cladding.

¹⁵ It should be noted that the ASME III requirements are largely accepted by the NRC regulatory position defined by the "General Design Criteria" in Appendix A of 10CFR50 "General Design Criteria".

¹⁶ There is, however, allowance taken for loss of load bearing volume due to general corrosion, and for the effect of an "industrial environment" on fatigue crack initiation.

¹⁷ Note that this is no longer the case, and that licensing of new reactor designs or the extension of life of current reactors requires a full analysis of all degradation phenomena.

Appendix B – Effect of environment on unstable crack propagation and fracture resistance (Peter Ford)

B.1 Introduction

Fracture resistance is a regulated part of reactor component design, and a brief discussion is appropriate in this appendix for two reasons. First, a decrease in fracture resistance (the extent of which depends of the microstructural details and increasing strength levels of the material) leads to a reduction in the critical dimensions of a crack that could propagate to failure of a defected component in an unstable manner²⁰. The second reason is more esoteric, albeit of significant practical impact, in that a decrease in fracture resistance at a crack tip may well increase the subcritical crack propagation rate for SCC. In this case (Figure B-1) the decrease in fracture toughness will not only reduce the crack dimensions required for unstable crack propagation, but may significantly increase the subcritical crack propagation rate and shorten the time before that instability occurs.

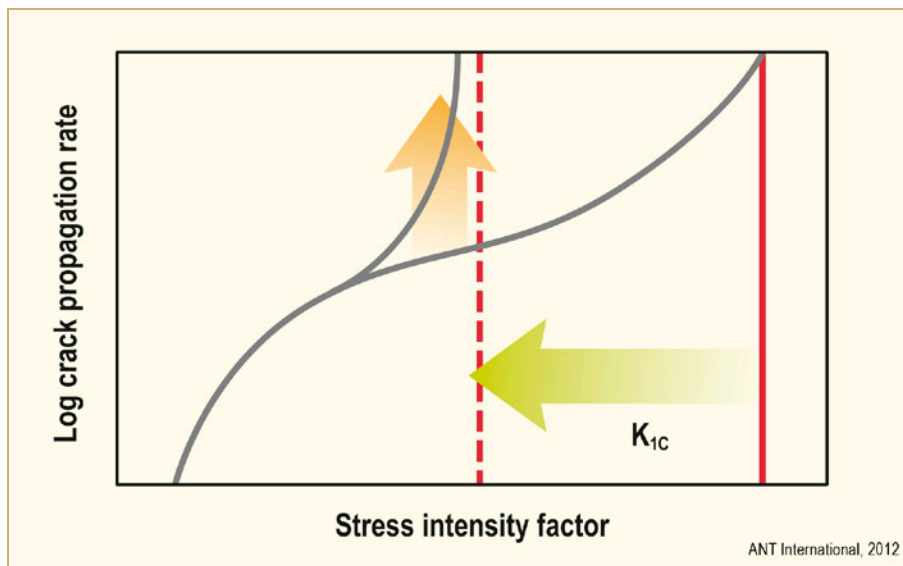


Figure B-1: Schematic crack propagation rate vs. stress intensity factor, illustrating the potential increase in subcritical SCC propagation rate (the orange arrow) associated with a decrease in the fracture resistance (the green arrow).

A detailed discussion of the development of Fracture Mechanics (FM) analyses and their use in the assessment of structural integrity of structural components in LWRs is outside the scope of this review; more detailed discussions are available elsewhere [Blinn & Williams, 1997], [Irwin, 1985], and [Knott, 1973]. However, a brief discussion is merited since FM analyses are widely used in discussions of EAC that are discussed in Chapter 5.

²⁰ “Unstable” in this context refers to the propagation of a crack at rates of the order of 350-400m/s.

For engineering applications, the linear elastic FM parameter most often used, particularly to correlate sub-critical SCC growth rates to component stability, as well as to characterize fracture resistance of relatively brittle materials, is the “stress intensity factor”, K , defined as:

$$\text{Eq. B-1:} \quad K = A \sigma \sqrt{\pi a}$$

Where “ σ ” is the stress, “ a ” is the crack depth and the factor “ A ” takes into account specimen size, shape and crack orientation with respect to the dimensions of the component and the principal stress directions.

Based on the original work of Griffith [Griffith, 1920] on brittle materials such as glass, and the subsequent developments by Orowan [Orowan, 1945] for more practical structural alloys, the fracture stress, σ_f associated with rapid unstable crack propagation is given by;

$$\text{Eq. B-2:} \quad \sigma_f = \sqrt{[E (2\gamma_s + \gamma_p) / \pi a]}$$

where $2\gamma_s$ is the surface energy associated with creating two crack surfaces, and γ_p is the energy associated with the plastic deformation at the crack tip. Rearranging Eq. B-1 and Eq. B-2 leads to the definition of the critical stress intensity factor, K_C , associated with specimen rupture²¹;

$$\text{Eq. B-3:} \quad K_C = A \sqrt{[E (2\gamma_s + \gamma_p)]}$$

Separate work by Irwin [Irwin et al, 1958] to justify in more rigorous terms the treatment of the energy associated with plasticity at the crack tip, led to the following relationship for K_C as a function of the crack depth and the yield stress, σ_y ²²;

$$\text{Eq. B-4:} \quad K_C = A \sigma_f \sqrt{[\pi a (1 + \sigma_f^2/2 \sigma_y^2)]}$$

Unstable crack propagation will occur for different combinations of stress and pre-existing crack dimensions [Shih, 1973] when K reaches a given critical stress intensity factor, K_C . However, care is required in quantifying such relationships especially when there is considerable plasticity at the crack tip. Under such conditions the assumptions of Linear Elastic Fracture Mechanics (LEFM) are violated. Thus, in the case of ductile alloys where a significant amount of crack tip plasticity may occur, alternate fracture assessment analyses, such as elastic-plastic approaches (Elastic-Plastic Fracture Mechanics (EPFM)) [Irwin, 1985], are appropriate. Consequently the American Society for Testing Materials (ASTM) have issued (and updated) standards for specimen dimensions and testing procedures that are appropriate for a given material metallurgical condition [ASTM, 1984], [ASTM, 1990], [ASTM, 1989], [ASTM, 1996] and [ASTM, 1993]. The ASTM has codified criteria for correlating the parameters that define unstable fracture under either LEFM (K_C) or EPFM (J_c), tearing modulus and crack tip opening displacement conditions.

It is important to point out, when discussing the interrelationships between subcritical crack propagation in Environmentally Assisted Cracking (EAC) and combinations of stress, crack dimensions, etc. that these fracture mechanics approaches are macroscopic analyses. In other words, they do not specifically take into account the microscopic details of the metallurgical conditions at the crack tip, such as the dislocation morphology and movement and the details of grain boundary embrittlement, etc. All of these microscopic factors may be important in defining the K_C value and, ideally, should be accounted for in any life prediction/structural integrity analysis.

²¹ Note that a roman numeral I, II or III may be included, (e.g. K_{IC}) to differentiate between differing loading modes; I for the opening mode (i.e. load applied perpendicular to the crack plane); II for in-plane shear, and III for torsion (or out of plane shear).

²² Note that Eq. B-4 takes into account the physical (e.g. surface energy) and mechanical (e.g. yield stress) parameters associated with unstable crack propagation. A more complete discussion would also include the energy associated with chemical reactions.

Appendix C – Corrosion of *ductile* austenitic alloys in LWR reactor internals (Peter Ford)

C.1 Introduction

Environmentally assisted degradation, especially that associated with irradiation, is a complex subject covering a wide range of phenomena spanning electrochemistry, physical metallurgy, mechanics, radiochemistry and irradiation damage, all of which interact in a non-linear fashion. A complete review would cover all the interactions (Figure C-1) between the material, environment and stress/strain conditions. For instance, interactions between the material and environment govern both; (i) uniform degradation, (experienced in general corrosion, boric acid corrosion and flow-accelerated corrosion), and; (ii) localized corrosion, (such as in galvanic attack, crevice corrosion, pitting and microbiologically-influenced corrosion). Interactions between the material and stress govern a number of phenomena, including fatigue and fracture resistance, while interactions between the (oscillating) stress and environment impact on phenomena such as corrosion fatigue. Finally, conjoint interactions between all three conditions (stress, environment and material) relate to environmentally-assisted cracking (EAC), which covers stress corrosion and hydrogen embrittlement, and is denoted by the shaded area in Figure C-1.

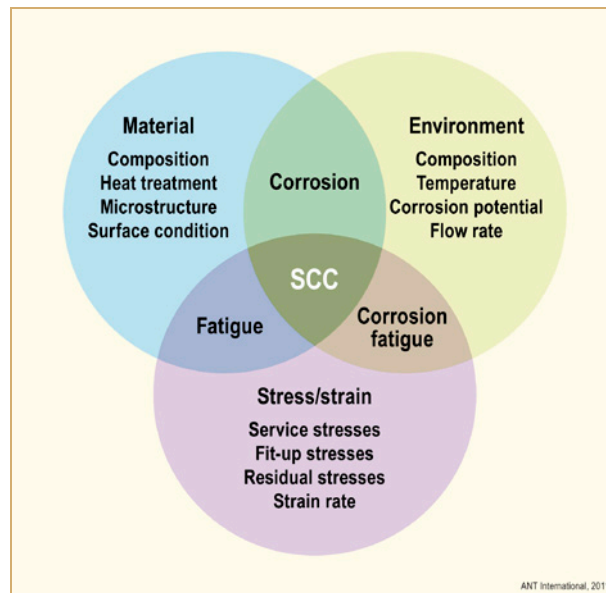


Figure C-1: Conjoint requirements for degradation of ductile alloys in LWRs.

Since the high-strength, high-nickel alloys are used in components that are easily replaceable (springs, etc.), there has been less research done to quantify all of these system interactions compared with that done on the *ductile* stainless steels [Ford et al, 2010] and nickel-base alloys [Scott et al, 2011], which are used for large passive structures.

However, as pointed out in Chapter 3 there is a spectrum of compositions (Table 3-1) (Figure 3-1) and physical metallurgical features for the high-strength high-nickel alloys that are bounded by those of the ductile austenitic stainless steels (e.g. Type 304) and Alloy 600. Thus the discussion logic is to give in this appendix a brief description of general corrosion and EAC of ductile Type 304 stainless steel and the nickel-base Alloy 600 in high temperature water relevant to BWRs and the primary circuit of PWRs. *This then acts as a framework for discussing and interpreting the data base for environmentally-assisted degradation of Alloys 286, 625, 718 and X-750 in Chapter 5.*

C.2 General corrosion of austenitic stainless steels and high-nickel alloys

C.2.1 Thermodynamic considerations

Corrosion of metals in aqueous environments involves various electrochemical and chemical reactions at, or close to, the material/environment interface. For instance, generalized reactions may be formulated for the electrochemical oxidation of a metal atom, M, to form either: (a), a solvated metal cation, M_{aq}^{n+} , (Reaction C-1); (b), a metal anion, MO_n^{n-} , (Reaction C-2) or, (c) an oxide, MO, (Reaction C-3). All of these reactions involve the release of electrons to the metal at the point of reaction on the metal surface, and, by definition, are described as electrochemical *oxidation* reactions.



There are, however, reactions that do not directly involve electron transfer; an example is the formation of an oxide via precipitation (Reaction C-4) which occurs when the solubility of the metal oxide is exceeded.



There are also reactions occurring on the metal surface which accept the electrons released by the oxidation reactions. These are defined as *reduction* reactions and are crucial since they are required in order to conserve charge on the metal surface. This point will be returned to in the discussion of the reaction kinetics and the concept of a corrosion potential, which is a key parameter in quantifying corrosion events.

The common reduction reactions in LWRs involve reduction of; (i) hydrogen cations (Reaction C-5); (ii) water (Reaction C-6) and; (iii) dissolved oxygen (Reaction C-7) or; other reducible species, such as hydrogen peroxide, cupric and ferric cations, etc.



in deaerated acid solutions, or the equivalent reaction



in deaerated neutral or alkaline solutions, or



in aerated solutions.

Under equilibrium conditions the change in Gibbs free energy, ΔG , associated with those surface reactions involving electron transfer (Reaction C-1-Reaction C-3, Reaction C-5-Reaction C-7), will have a value that is a function of temperature, metal cation or anion activity (for Reaction C-1 and Reaction C-2), oxygen concentration (Reaction C-7) and pH (for Reaction C-2, Reaction C-3, Reaction C-5-Reaction C-7). Moreover, since these reactions involve charge transfer and separation, the change in Gibbs free energy will be related to an electrode potential, E , at that surface (Eq. C-1), which is also a function of the concentration of the oxidized state (e.g. H^+) and reduced state (e.g. H_2) via the Nernst equation (Eq. C-2);

$$\text{Eq. C-1:} \quad E = -\Delta G/nF$$

$$\text{Eq. C-2:} \quad E = E_0 + RT/nF \cdot [\ln [\text{oxidized state/reduced state}]]$$

where F is Faradays constant (96500 coulombs/ equivalent), and n is the number of electrons exchanged in the reaction and E_0 is the standard electrode potential.

The stability of the precipitated oxide in Reaction C-4 will be dependent on the interactions between temperature, pH_T and oxide solubility. Since the reaction does not involve electron transfer, the stability of the precipitated oxide is independent of potential.

The reader is referred to other ANT International reports [Ford, 2006], [Ford & Scott, 2008], [Ford et al, 2010], [Scott et al, 2011], and standard corrosion and electrochemistry text books for details of these electron transfer relationships as they apply to specific metal/water systems, and the derivation (and measurement) of the electrode potential that exists at the metal/solution interface.

These basic concepts lead to the construction of a Pourbaix diagram [Pourbaix, 1974] which denotes the potential/ pH_T combinations where various species (M , MO , M_{aq}^{n+} , MO_n^{n-}) are thermodynamically stable or metastable at a given temperature. The electrode potential/ pH_T Pourbaix diagram for nickel in water at 300°C is shown in Figure C-2a where the stability regions are indicated for the base metal (Ni), dissolved cations (Ni^{2+}) and anions ($\text{H}\text{Ni}_2\text{O}^-$) and oxides (NiO , Ni_3O_4 , Ni_2O_3 , NiO_2). This presentation of information is often shown as Figure C-2b where the E/pH_T combinations for “immunity”, “passivation or protective film formation”, and “active corrosion” are denoted by coloured regions²⁵.

The observed electrode potential for a given metal in contact with water is governed by the fact that, in order to maintain electroneutrality, the sum of all oxidation reaction rates at that surface must equal the sum of all of the reduction reaction rates. The electrode potential at which that equality is reached is the “Electrochemical Corrosion Potential” (ECP). A significant factor for the structural alloys used in high temperature water (above 150°C) is that the metal oxidation rates (Reaction C-1, Reaction C-2, Reaction C-3) are much lower than the oxidation and reduction rates for the dissolved hydrogen, oxygen (and hydrogen peroxide) (Reaction C-5 and Reaction C-7). The result is that the ECP of the metal surface is governed predominately by balancing the oxidation rate for H_2 and the reduction rate of O_2 (or H_2O_2), regardless of structural alloy composition. Thus, as indicated in Figure C-3, the corrosion potential for stainless steels is a function of the temperature, and the dissolved hydrogen peroxide, oxygen and hydrogen fugacities. Very similar ECP vs. O_2 , H_2O_2 , T and H_2 relationships are observed for the carbon and low alloy steels, nickel-base alloys and stainless steels.

There are two consequences of this vis. a vis. the stability of the various phases at the metal/environment interface:

- If two dissimilar alloys are connected there will be little chance of galvanic attack, since the ECP for both alloys will be the same²⁶.
- The ECP for LWR structural alloys will be limited in oxidizing environments by the reversible potential for Reaction C-7 given by (line b) in Figure C-2a and by the H^+/H_2 redox reaction (Reaction C-5) given by line (a).

This latter point is illustrated in Figure C-4 by the Pourbaix diagram for the Ni/water system at 300°C where the ranges in observed ECP values for nickel-base alloys have been inserted for BWR Normal Water Chemistry (BWR-NWC), BWR Hydrogen Water Chemistry (BWR-HWC) and PWR Primary system conditions (PWR-primary). It is noteworthy that the ECP for nickel-base alloys in PWR primary environments is governed by the redox potential for H_2/H^+ equilibrium, and that this is close to the Ni/NiO equilibrium potential. Thus Ni or NiO may be stable depending on the H_2 fugacity and temperature. This, as will be seen later, is of significance to SCC of nickel-base alloys at these low corrosion potentials.

²⁵ Note that the Pourbaix diagram indicates what species *cannot* exist thermodynamically at a given E/pH combination. The converse is not true, however, for although a species may be thermodynamically stable, its presence may be restricted due to kinetic reasons.

²⁶ Note that this does not minimize problems with dissimilar metal joints due to physical metallurgical and residual stress issues, nor does it ignore potential galvanic problems at temperatures below approximately $150\text{-}200^\circ\text{C}$ due to the increased oxidation rate of carbon and low alloy steels.

Appendix D – References

- Airey G. P., *The stress corrosion cracking (SCC) performance of Inconel Alloy 600 in pure and primary water environments*, Proceedings of 1st International Symposium on Environmental Degradation of Materials in Nuclear Power Systems-Water Reactors, pp. 462-476, National Association of Corrosion Engineers, 1984.
- Akashi M and Nakayama G., *Effect of acceleration factors on the probability distribution of SCC initiation life of Alloys 600, 182 and 82 in high temperature and high purity water environments*, in Proceedings of 9th Conference on Degradation of materials in Nuclear Power systems, Newport Beach, CA, 1999.
- Amzallag C. and Vaillant F., *Stress corrosion crack propagation rates in reactor vessel head penetrations in Alloy 600*, Proceedings of 9th International Symposium on Environmental Degradation of Materials in Nuclear Power Systems – Water Reactors, pp. 235-241, Newport Beach, CA, The Metallurgical Society, 1999.
- Amzallag C., Le Hong S., Pages C. and Gelpi A., *Stress corrosion life assessment of Alloy 600 components*, Proceedings of 9th International Symposium on Environmental Degradation of Materials in Nuclear Power Systems – Water Reactors, pp. 243-250, Newport Beach, CA, The Metallurgical Society, 1999.
- Amzallag C., Boursier J-M, Pages C. and Gimond C., *Stress corrosion life assessment of 182 and 82 welds used in PWR components*, Proceedings of 10th International Conference on Environmental Degradation of Materials in Nuclear Power Systems-Water Reactors, Lake Tahoe, August 5-9, 2001, NACE International, 2002a.
- Amzallag C., Boursier J-M., Pages C. and Gimond C., *Stress corrosion life experience of 182 and 82 welds in French PWRs*, Proceedings of Fontevraud 5, pp. 69-79, SFEN, 2002b.
- Andresen P. L., *Effect of Material and Environmental Variables on Stress Corrosion Crack Initiation in Slow Strain Rate Tests on Type 304 Stainless Steel*, Symp. On Environmental Sensitive Fracture; Evaluation and Comparison of Test Methods, April 1982. Published in ASTM STP821 pp. 271-287, 1984.
- Andresen P. L., *Modelling of water and material chemistry effects on crack tip chemistry and resulting crack growth kinetics*, Proceedings 3rd Int. Conf. Environmental Degradation of Materials in Nuclear Power Systems - Water Reactors, Traverse City, AIME, pp. 301-314, 1987.
- Andresen P. L., Ford F. P., Murphy S. M., Perks J. M., *State of knowledge of radiation effects on environmental cracking in light water reactor core materials*, pp. 1-83 to 1-121, Proceedings of the 4th Conference on Environmental Degradation of Materials in Nuclear Power Systems – Water Reactors, Jekyll Island, GA, August 1989.
- Andresen P. L., Vasatis I. and Ford P., *Behaviour of short cracks in stainless steel and Inconel in 288°C water*, Paper 495, Corrosion/90, NACE, Houston 1990.
- Andresen P. L., *Effects of Specific Anionic Impurities on Environmental Cracking of Austenitic Materials in 288°C Water*, in Proceedings of Fifth International Symposium on Environmental Degradation in Nuclear Power Systems – Water Reactors. Monterey August 25-29, 1991, Eds. D. Cubicciotti, E. Simonen, Published, by American Nuclear Society, ISBN 0-89448-173-8, pp. 209-218, 1991.
- Andresen P. L., *Effect of Temperature on Crack Growth Rate in Sensitized Type 304 Stainless Steel and Alloy 600*, Paper 89 NACE Corrosion -92, Nashville, April 1992.
- Andresen P. L. *Specific Anion and Corrosion Potential Effects on Environmentally Assisted Cracking in 288°C Water*, GE-CRD Report 93CRD215, December 1993a.